UNIVERSITY OF CENTRAL OKLAHOMA

Edmond, Oklahoma

Jackson College of Graduate Studies

The Biosynthesis Reaction of Hypotaurine to Taurine

A THESIS

SUBMITTED TO THE GRADUATE FACULTY

In partial fulfillment of the requirements

For the degree of

MASTER OF SCIENCE IN BIOLOGY

By

Roxanna Q. Grove

Edmond, Oklahoma

2018

The Biosynthesis Reaction of Hypotaurine to Taurine

A THESIS

APPROVED FOR THE DEPARTMENT OF BIOLOGY

March 2018

By Nikki Seagraves

Name Committee Chairperson

Lilian Chooback June 19, 2018

Name Committee Member

Steven Karpowicz

Name Committee Member

Name Committee Member

Acknowledgments

Working on this project has been a period of intense learning for me, not only in the scientific arena, but also on a personal level. Writing this thesis has had a significant impact on me. I would like to reflect on people who have been supported and helped me so much throughout this period.

First of all, I would like to express my gratitude toward my advisor, Dr. Steven J. Karpowicz, for his devotion, inspiration, and guidance. I am so grateful to have the opportunity to work with such an intelligent, dedicated, and patient professor. I appreciate his vast knowledge and skills in many areas such as biochemistry, genetics, and bioinformatics, and his assistance in writing this thesis.

I would like to thank the other members of my committee, Dr. Nikki Seagraves, Dr. Hari Kotturi, and Dr. Lilian Chooback, for their guidance, support, and for providing materials throughout this project. An exceptional thanks go to Dr. John Bowen of the Department of Chemistry for advice in the analytical laboratory and Dr. Susan L. Nimmo from the Department of Chemistry and Biochemistry at the University of Oklahoma for assistance with NMR.

This project was supported by funding from the College of Mathematics and Science and a Research, Creative, and Scholarly Activities (RCSA) grant from the Office of High Impact Practices at UCO.

Finally, I would like to express my profound gratitude to my husband Timothy Grove for providing me with unfailing love, support, and continuous encouragement throughout my years of study and through the process of researching and writing the thesis.

ABSTRACT OF THESIS

University of Central Oklahoma

Edmond, Oklahoma

NAME: Roxanna Q. Grove

TITLE OF THESIS: The Biosynthesis Reaction of Hypotaurine to Taurine

DIRECTOR OF THESIS: Steven J. Karpowicz, Ph.D.

PAGES: 118

ABSTRACT:

Taurine (2-aminoethanesulfonic acid) is one of the most abundant amino acid-derived molecules in humans and most eukaryotes. Despite its many roles and functional properties, the biochemical mechanisms and the reaction of hypotaurine to taurine are still unknown. This study focuses on the biosynthesis reaction of hypotaurine to taurine *in vivo* and *in vitro* by using bioinformatics tools, enzymatic assays, and analytical techniques.

Transcriptional co-expression analysis of 26 tissue and organ samples revealed Flavin- Monooxygenases (FMO) that seemed to be suitable candidates to catalyze the reaction of hypotaurine to taurine. However, enzymatic assay showed no chemical reaction on HPLC analysis after adding cofactors NAD^+ and NADPH to HuH 7 hepatoma cells and 11 day-old embryonic chicken livers. Enzymatic assays failed to confirm an enzyme for the reaction of hypotaurine to taurine.

Analytical assays were used to determine the spontaneous reaction of hypotaurine to taurine with Reactive Oxygen Species (ROS). HPLC, ESI-MS, NMR, FTIR and

Raman assays were applied to investigate the reaction of hypotaurine and taurine with ROS such as superoxide, hydrogen peroxide, and singlet oxygen. HPLC and ESI-MS tests confirmed that hypotaurine did not react with singlet oxygen. However, various tests confirmed that hypotaurine reacted with hydrogen peroxide and superoxide. Analytical assay results revealed a novel molecule in the reaction of hypotaurine or taurine with superoxide. FTIR, NMR and Raman spectroscopy confirmed the characteristics of the novel molecule, peroxytaurine. Chemical methods to detect the peroxide in peroxytaurine was attempted with acridine, pyridine, and iron.

Table of Contents

Chapter 1

Introduction and Background

I. Introduction

Taurine (2-aminoethanesulfonic acid) is an organic compound with the chemical structure $C_2H_7NO_3S$ (Figure 1.1). It is usually mischaracterized as an amino acid although it contains a sulfonic acid group rather than a carboxylic acid group [1]. Technically, it is a sulfonic acid that also contains an amino group. Taurine is one of the most abundant amino acid-derived molecules in cells, and it is implicated in multiple physiological and biological functions [2]. It is ubiquitous in animal tissues in the range of 1 to 50 mM, although it is highly concentrated in neutrophils, liver, brain, eye, heart and skeletal muscles. Taurine constitutes 0.1 percent of adult human body weight [3]. It forms a colorless crystal compound as a solid and has a molecular weight of 125.15 g/mol. Taurine is soluble in water but almost insoluble in ethanol and ether. Both active groups in taurine, the sulfonic acid and the amine, may be ionized. Taurine is a zwitterion at pH 7.4, and it is highly hydrophilic with low lipophilicity. The pK_a values of taurine at 25°C have been determined to be 1.5 for the sulfonic acid and >9 for the amine [4]. It is the end-product of the metabolism of cysteine and other biological molecules.

Stipanuk *et al*. [5] provided a detailed assessment of how the processes resulting in taurine production operate. Taurine synthesis occurs in the liver via a cysteine sulfinic acid pathway. In human beings, taurine is produced in hepatocytes. L-cysteine is oxidized to cysteine sulfinic acid by the enzyme cysteine dioxygenase. Other analyses identify how taurine production operates within the liver, specifically. Stipanuk *et al*. [6] observed that taurine-specific metabolism takes place in the liver and that the liver is the first organ

to respond to the influx of sulfur amino acids from meals, disposal of sulfur amino acids, and release of taurine and glutathione into plasma. The enzymes cysteine sulfinate decarboxylase (CSAD) and cystamine dioxygenase (ADO) activities are identified more frequently in the liver than in other tissues [7].

Initially, taurine was isolated from ox bile by two German scientists, Leopold Gmelin and Friedrich Tiedemann, in the year 1827. Yancey *et al.* [8] noted that within many mammal species, taurine is a conditionally essential amino acid-derivative during fetal development. It is viewed as a non-essential nutrient in rodents, but an essential nutrient in cats. Other research seeks to differentiate taurine production processes in humans from other mammals. Sturman and Gaull [9] studied the concentration of taurine in humans and monkeys throughout the gestation, birth, and neonatal life. Their study showed that the taurine concentration was 2-fold higher in the human fetal liver than in the mature human liver. After birth, the level declined and remained the same for the rest of the lifetime. It indicated that the potential gene is on and highly active during the fetal developmental stage and suppressed after birth. Newborn mammals are unable to synthesize a sufficient amount of taurine and have to rely on dietary supply. The human infant obtains taurine from mother's breast milk. Human milk contains a high-level concentration of taurine. Those who do not receive mother's milk require food with taurine supplementation. Taurine deficiency in the embryo is associated with consequences such as growth retardation, retinal degeneration, and cardiomyopathy [10]. Taurine deficiency in neonates causes deleterious effects on retina and brain development. Excessive taurine deficiency can also result in certain rare diseases such as cardiomyopathy, renal dysfunction, developmental abnormalities and retinal neurons

damage. Taurine concentrations can be measured in blood plasma and urine. Full-term infants showed a substantially higher-level concentration of taurine in urine than premature infants [4]. Humans have a low capacity to synthesize taurine after birth and must rely on intestinal uptake from meat and seafood. Vegans show a low concentration of taurine.

The primary dietary sources of taurine in healthy humans are mainly from meat, seafood, egg, and milk. There is no, or negligible taurine content detected in cereals, peanuts, beans, grains, nuts, seeds, fruits, and vegetables. Hence, vegetarians have lower plasma concentrations of taurine. Its primary precursor is cysteine, although the ability to synthesize taurine widely varies among species. An adult human synthesizes an average of 0.4 to 1.0 millimolar of taurine per day. Under stress, the synthesis of taurine in humans can be impaired. Hence, taurine may be regarded as a conditionally-essential amino acid derivative [11].

Since taurine is involved in the process of bile acid conjugates, deficiency of taurine plays a part in the pathogenesis of cholestasis, a condition where bile cannot flow from liver to the duodenum. Taurine supplementation altered the pattern of secretion and conjugation of the bile acid to facilitate the bile flow and prevent hepatotoxic bile acids stasis [11].

Taurine plays a crucial role in detoxification, osmoregulation, intracellular calcium level modulation, and cell membrane stabilization. It can regulate many physiological functions that can alternate due to a variety of clinical conditions [12]. Despite that its mechanism of action is not comprehended, taurine seems to have essential cardiovascular effects as well as influences central nervous system (CNS)

neuromodulation, platelet aggregation, retinal photo-receptor activity, antioxidant activity, endocrine functions, cell growth and differentiation.

II. Biosynthesis of Taurine

Endogenous synthesis of taurine mainly occurs in the liver via multiple steps involving oxidation by enzymes as illustrated in Figure 1.2. Dietary methionine can be metabolized to cysteine and cysteine is the precursor for taurine [13]. The enzymes involved in the pathway of conversion from cysteine to taurine are cystamine dioxygenase (ADO), cysteine dioxygenase (CDO1), cysteine sulfinate decarboxylase (CSAD), glutamate decarboxylase (GAD), and glutamine decarboxylase-like (GADL). Two of the enzymes of the cysteine metabolism pathway, cystathionine synthase and γ-cystathionase, and the taurine pathway enzyme CSAD require the cofactor pyridoxal 5' phosphate (vitamin $B_{6)}$) for full enzymatic activity. Dietary deficiency of vitamin B_6 can lead to taurine depletion due to reducing taurine synthesis [14, 15].

In humans, taurine is produced in hepatocytes from methionine and cysteine through hypotaurine. L-cysteine is derived from methionine and serine. L-cysteine is oxidized to cysteine sulfinic acid by enzyme cysteine dioxygenase (CDO1). Cysteine sulfinic acid is then decarboxylated by the enzyme cysteine sulfonate decarboxylase (CSAD) to form hypotaurine. The conversion of hypotaurine to taurine was still unclear at the beginning of this thesis projects.

In astroglial cells, the pathway of conversion of hypotaurine to taurine seems rather slow. Hypotaurine is the main product of metabolism of cysteine in astroglial cells. Brand *et al*. [16] hypothesize that there is the possible movement of the two vital organic osmolytes, hypotaurine and taurine, to the neurons from the astrocytes. Synthesis of

hypotaurine in the neurons from cysteine is quite unlikely since the localization of the enzyme cysteine sulfinate decarboxylase, which is essential for this role, is in the astrocytes rather than in the neurons. Hence, as suggested by Brand *et al.* [16], the hypotaurine generated in the astrocytes may act as a precursor for taurine synthesis within the neurons of other brain cell types.

III. Distribution of taurine

Taurine is not incorporated into the body's proteins. Only a small proportion of it occurs in the brain as small peptides such as glutamyl-taurine [17]. It is mostly free in solution and is found in high concentration in cells and tissues like platelets, white blood cells, retina, liver, central nervous system, brain, skeletal muscle, and heart, which are prone to produce oxygen free radicals [18]. Taurine is involved in multiple biochemical reactions although one significant physiological role is the protection of cell membranes by osmoregulation or through amelioration of the effects of toxic substances [19]. Taurine is transported actively to all tissues in the body through a membrane transporter SLC6A6, which is coupled to the transport of chloride and sodium ions. Taurine transport is controlled by the activation of inhibitory and stimulatory enzymes of SLC6A6, which are identified as a protein kinase and calmodulin, respectively [13].

While the excretion of taurine occurs in the bile or urine, its total pool in the body is regulated in the kidney through altering reabsorption in its tubules. Taurine is filtered via the glomerulus then partial reabsorption occurs within the tubules via a high-affinity, low-capacity, sodium-dependent, β-amino acid specific transport system [20]. The daily amount of excreted taurine varies from one person to another and within the same individual daily depending on such factors as age, current dietary intake, sex, renal

function, or certain clinical conditions. An individual with dysfunctional renal tubules is at elevated risk of taurine deficiency. Renal reabsorption of taurine increases in cases of insufficient dietary intake and inadequate precursor amino acids, to favor the maintenance of tissue stores [20]. On the other hand, renal excretion of taurine is increased in the case of high dietary intake, radiotherapy, and any conditions which induce the release of taurine from cells, like muscle damage, disease, or surgery.

IV. Taurine Bacterial Degradation

Animals or plants are not known to have a pathway to degrade taurine. However, taurine can be degraded by multiple species of bacteria and potentially some fungi. Certain anaerobic bacteria may use taurine as an electron donor or receptor. Some other bacteria may use taurine as a substrate for fermentation [21]. These variant species use separate pathways leading to a breakdown of taurine into several distinct compounds. Three known reactions initiate degradation of taurine are transamination [22], oxidation, [23] and oxygenation, [24]. In both oxidation and transamination, the intermediate is sulfoacetyladehyde, while, in the case of oxygenation, taurine is broken down into aminoacetaldehyde and sulfite.

Alcaligenes defragrans NKNTAU, an aerobic bacterium, converts taurine into sulfoacetyladehyde that is then broken down to sulfite and acetyl phosphate, and then finally converted by a sulfite reductase into hydrogen sulfide. Taurine acts as an electron donor in respiration for *Alcaligenes defragrans* NKNTAU, *Paracoccus pantotrophus* NKNCYSA, and *Paracoccus denitrificans* NKNIS to produce sulfate, ammonia and carbon dioxide (CO_2) [25].

Anaerobic bacteria have a broad range of dissimilatory reactions with taurine. Taurine serves as an electron acceptor with *Bilophila wadsworthia* RZATAU to yield hydrogen sulfide, ammonia, and acetate. Taurine also acts as a fermentative substrate for *Desulfonispora thiosulfatigenes* GKNTAU to yield thiosulfate, acetate, and ammonia [21].

Dissimilation of taurine involves two main aminotransferase enzymes: taurine-pyruvate aminotransferase, found in both anaerobic and aerobic bacteria, and taurine α-ketoglutarate aminotransferase. The enzyme taurine α-ketoglutarate aminotransferase is induced by β-alanine and, hence, its main physiological role is β-alanine transamination [21]. By the activity of the enzyme taurine-pyruvate aminotransferase, the amino group is transferred from taurine to pyruvate to form L-alanine. The oxidative deamination of alanine is catalyzed by alanine dehydrogenase to form pyruvate, as well as the release of ammonium [26].

V. Bio-Physiological functions of Taurine

A. Conjugation of bile acid and deterrence of cholestasis

Chenodeoxycholic and cholic bile acids are produced from cholesterol within the hepatocytes via the enzymatic action of cholesterol 7-α-hydroxylase and then excreted as bile into the duodenum [11]. The secondary bile acids, lithocholic and deoxycholic acid, are synthesized from the primary bile acids through their contact with bacteria in the intestines, then the ileum reabsorbs the bile acid through the portal vein into the liver. Bile acids go through multiple structural modifications during enterohepatic circulation such as conjugation with glycine or taurine, as well as sulfation, to decrease the bile acids' hepatoxicity. Furthermore, conjugation is very important in the maintenance of

solubility of bile acids in the aqueous environment of the intestines.

In healthy adults, the ratio of glycine-conjugated vs. taurine-conjugated bile acids is 1:3. The hepatic taurine pool influences this ratio, and it varies from one individual to another. Newborn infants are exclusive taurine-conjugators [27]. Glycine conjugation is usually absent up to the third week of life although earlier appearance may be observed in taurine-deficient newborns.

In vitro, at physiological concentrations, sulfated glycolithocholate is precipitated readily by calcium, while conversely, sulfated tauro-lithocholate stops calcium precipitation and cholestasis. Supplementation of taurine facilitates the activity of hepatic enzyme cholesterol 7-α-hydroxylase, which is the enzyme that limits the rate of bile acid synthesis [28].

B. Taurine in Mitochondrial tRNA

Despite decades of research, aspects of the function of taurine remain unknown. One of the emerging areas of research in the field relates to the role that taurine has in mitochondrial tRNA in human and mammalian biochemistry. Understanding the role of taurine in mitochondrial tRNA also can be potentially helpful for identifying a link between taurine production and deficiencies and presently untreatable diseases.

Suzuki *et al*. [29] identified two taurine-containing modified uridine residues in mitochondrial tRNA: 5-taurinomethyluridine and 5-taurinomethyl-2-thiouridine. The taurine-containing uridines are located at the anticodon wobble position of human and bovine mt $tRNA^{Leu}$(UUR) and mt $tRNA^{Lys}$. This study provided the first evidence that showed that taurine is a constituent of biological macromolecules and revealed insights into the functions and subcellular localization of taurine. The identity of the taurine-

containing modified uridines yields an important discovery that enhances our knowledge of the diversity and centrality of taurine within mitochondrial structures. The study suggested that due to the role of mitochondrial tRNA, taurine may play a significant role in the translation and expression of the mitochondrial respiratory proteins. Taurine`s notable impact upon mitochondrial structures might potentially be applied in human diseases from affected mitochondrial functions and the loss of a post-transcriptional modification. Pathogenic cells from patients with mitochondrial myopathy, encephalopathy, lactic acidosis, and stroke-like episodes (MELAS) were shown missing 5-Taurinomethyl uridine (τm^5U) at the wobble position in the mt tRNA. This decoding was due to lack of C5 taurine modification. The authors suggested that incomplete modification of 5-Taurinomethyl 2-thiouridine (τm^5s^2U) in mt tRNAs due to a low plasma taurine level may be the primary factor that causes cardiomyopathy in cats and mitochondrial encephalomyopathies in humans.

Hansen *et al*. [30] claimed that taurine's pK_a value is ideal for controlling the metabolic activity of the Acyl-CoA dehydrogenase (ACAD) enzymes and functions as an optimal mitochondrial matrix buffer. Depletion of intracellular taurine is associated directly with mitochondrial dysfunction and causes insufficient pH buffering of the matrix. The intracellular accumulation of carbohydrates, lipids, and polyols cause diabetes and metabolic syndrome, which the authors claim to imply taurine deficiency. The research indicates the potential link between low taurine levels in a patient`s system and hyperglycemia. This observation may also help yield advances in medical research that can address the diabetes pathology by administering taurine to affected structures.

C. Cardiovascular effects

Taurine is found to have a high concentration in the cell cytosol and is abundant in heart and plasma [31]. Taurine is demonstrated to have optimal inotropic (increasing or decreasing the force of muscular contractions), antiarrhythmic, and chronotropic (influencing the rate of the heartbeat) effects in the facilitation of digitalis inotropy, plus it can lower blood pressure in humans as well as other eukaryotes. Chen *et al*. [32] demonstrated that taurine improves cardiac function by reducing the protein oxidation levels in mitochondria of methionine sulfoxide reductase A (MsrA) gene knockout mice.

D. Taurine in central nervous system

Taurine is the most prevalent amino-derived molecule in the brain [33] and has a high concentration in fetal brain but decrease in adults [34]. The high concentration of taurine in fetal brain suggested that it plays an essential role in brain development. An experiment by Hernández-Benítez *et al*. [34] showed that taurine has a stimulatory effect on neural progenitor cells, which showed an increase of neurosphere size and cell numbers. In addition, taurine also functions as an osmoregulatory and neurotransmitter in the brain [35].

E. Neuro-modulation of the central nervous system

Taurine is localized within the central nervous system and in the brain, affects migration of cells, and regulates neurotransmission. By controlling calcium ion mobilization during membrane depolarization, taurine stabilizes membranes and alters the excretion of glutamate, which is an essential neurotransmitter. The studies were undertaken by Cunningham and Miller [36] about taurine action on neuronal pathways in the retina of the rabbit show that taurine is capable of separating the ‘on’ and ‘off’

channels of certain cell signaling pathways. These pathways were observed by extracellular electrophysiological recordings electroretinogram (ERG) and proximal negative response (PNR), and intracellular recorded Müller cell responses.

Taurine deficiency results in delays in differentiation or migration of cells within the cerebellum, pyramidal and visual cortex cells in monkeys and cats. Furthermore, Hernandez-Benitez *et al*. [37] demonstrated that taurine facilitates the development of neurons in both brains of adults and embryos. Taurine activates neural precursor cells and stems cells' differentiation to neurons in the subventricular zones of cultured adult mouse brains. This zone is amongst the few brain regions in which neurogenesis progresses all through adulthood. Its cells can proliferate or migrate into the olfactory bulb for differentiation into neurons through the rostral migratory stream [20]. The high content of taurine in the adult olfactory bulb can be considered to implicate taurine's significance in neurogenesis.

F. Retinal photoreceptor activity

The retina has a high concentration of taurine ranging from 10 to 50 mM. It seems essential for normal vision. Taurine deficiency has been linked to failure for photoreceptors to mature correctly and photoreceptor degeneration in the adult retina [38]. Moreover, photoreceptors are rich in taurine compared to other retinal neurons. Apparently, taurine plays a part in neuroprotection in the ganglion cells and the photoreceptors as well. However, Miller and Steinberg [39] learned that *in vivo* experiments on taurine's active transport showed that the main flux was in the retina towards the choroid coat, thickest at the far extreme rear of the eye. Conversely, Hillenkamp *et al.* [40] established that if a small molecule like taurine passively diffuses,

then it can go across the plasma membrane of the retinal cells with no help of the mechanism for active transport. The directionality of taurine transport across the retinal pigment epithelium (RPE) is driven by the taurine concentration gradient and subretinal potassium level. Reduction in apical potassium leads to the decrease in taurine transport across Bruch's choroid and RPE. Aging human retina and retinal disease exhibit taurine deficiency.

Deficiencies of taurine are linked to degeneration of the retina. For instance, taurine in cats is considered an essential nutrient. If there is a deficiency of taurine, degeneration of the retina and subsequent blindness alongside low plasma and retinal concentrations will result. In newborn monkeys, insufficiency of taurine is linked to growth retardation while retinal function appeared not impaired. Taurine deficiency in primates is associated with degenerative structural changes in the outer segments of the photoreceptor, retinal lesions, and diminished visual acuity [13].

Taurine is present at high levels during the developmental stage in mammals. During infancy, children who are reared on parenteral nutrition without taurine exhibit immature brain stem, auditory, and retinal abnormalities. These effects were observed through electrophysiology and ophthalmoscopy. Signal reduction of the b-wave was seen from the electroretinogram, linked to reduced concentrations of taurine in plasma. After taurine supplementation, then the electroretinogram normalized [40]. However, there is still no precise mechanism, although inhibition of protein phosphorylation or changes in osmoregulation and modification of calcium ion fluxes might be involved.

G. Endocrine and metabolic effects

Taurine plays a role in maintaining euglycemia through enhancement of insulin

activity by increasing glycogen synthesis in the liver and taurine insulin-receptor interaction [41]. In diabetes mellitus, low platelet and plasma taurine levels are observed while supplementation with taurine has been reported to restore both plasma taurine concentrations and increase kinin, hence increase kallikrein activities in liver, kidney, and heart [42]. In a rat model that had diabetes, studies revealed taurine buffered the level of glucose and rate of fat metabolism alongside reduced resistance to insulin [43]. The reduced triacylglycerol and cholesterol content may result in a more significant transformation of cholesterol in the bile acids as well as declined cholesterol synthesis. Therefore, taurine may aid in managing human hypercholesterolemia.

Also, taurine may hinder microangiopathy, which is associated with diabetes. Taurine appears to decrease apoptosis of the hyperglycemia-affected endothelial cells by inhibiting reactive oxygen species and stabilizing concentrations of intracellular calcium [44].

H. Antioxidant Activity

Aruoma *et al*. [45] suggest that taurine can act as an oxidant scavenger or antioxidant. Hypotaurine, taurine, and their metabolic precursors - cysteine-sulfinic acid, cysteic acid, and cysteamine - play an antioxidant role *in vivo* [46]. However, taurine does not rapidly react with $^{\bullet}OH$ and H_2O_2. Additionally, the product of taurine's reaction with a hypochlorous acid (HOCl) is taurine chloramine. HOCl is a robust oxidizing agent that causes damage to DNA. Taurine chloramine may have a modulatory action in inflammatory processes by inhibiting the generation of interleukin 8 (IL-8) and IL-6, due to reduced activity of the primary transcriptional cytokine gene modifiers [47]. Taurine

chloramine is sufficiently oxidizing to deactivate alpha 1-antiproteinase. Hence, *in vivo*, taurine is not a potent antioxidant.

On the other hand, hypotaurine is an excellent hypochlorous acid (HOCl) and hydroxyl radical ($^{\bullet}OH$) scavenger *in vivo*. It can also interfere with the iron ion-dependent formation of $^{\bullet}OH$ from hydrogen peroxide (H_2O_2) by chelating iron ions. Also, cysteamine reacts actively with H_2O_2, HOCl and $^{\bullet}OH$ *in vivo* [45]. Therefore, both hypotaurine and cysteamine are more potent antioxidants *in vivo* than taurine, as long they are available in adequate concentrations at oxidant generation sites.

In hamsters, acute bronchiole injury induced by NO_2 and lung injuries caused by oxidants may be prevented by prophylactic dietary taurine. The damage can be reversed through the ability of taurine to stabilizing the membrane by promoting magnesium, calcium, sodium and potassium fluxes [48].

Taurine plays a significant role in inflammation associated with oxidative stress by reacting with and detoxifying hypochlorous acid that is generated by the myeloperoxidase (MPO)-halide system of leukocytes [49]. Finally, taurine overwhelms glutamate-induced toxicity via multiple mechanisms: a) by inhibiting calcium influx via Q-, P-, N- and L-type voltage-gated calcium pathways, b) by protecting neurons from oxidative stress, c) preventing up-regulation of Bax and down-regulation of Bcl-2 protein product that would otherwise migrate to the mitochondria and cause a release of cytochrome *c*, which is highly toxic, and d) by inhibiting activation of glutamate-induced calpain and preventing the cleavage of Bcl-2 [50].

VI. Taurine in cats

Taurine deficiency can affect cats' eyesight. Cats that eat a vegetarian diet, in

which taurine is absent, or cooked meat, in which taurine is degraded, become blind over ten weeks. It is possible that cats cannot synthesize sufficient quantities of taurine to compensate for the use of taurine in bile acids.

Humans and other vertebrates can conjugate glycine to bile acids when the taurine concentration is depleted. Cats cannot switch the conjugation from taurine to glycine [14]. The dietary absence of taurine in adult and juvenile cats can cause effects on ganglion cell activation and lead to the loss of function in retinal cells [51]. Low taurine concentration in the outer retina can produce signs of deterioration in the photoreceptors, as observed by electron microscopy, which leads to central retinal degeneration and eventually irreversible blindness [3].

Schuller-Levis *et al*. [52] conducted an intensive study that contrasted the immunological impact on cats that were fed a taurine-rich diet and those that were deliberately deprived of taurine. Their experiment indicated that cats that were fed a diet lacking in taurine showed significant leukopenia, which is an increased count of white blood cells, and a shift in the percentage of polymorphonuclear and mononuclear leukocytes. Serum gamma globulin in taurine-free diet cats was significantly increased compared to a taurine-rich diet. Histological examination of lymph nodes and spleen from cats fed a taurine-free diet showed mild extravascular hemolysis and regression of follicular centers with depletion of reticular cells. These results indicated the profound immunologic impact caused by taurine deficiency.

Froger *et al.* [15] found that taurine may have a positive impact on human retinal diseases such as glaucoma and diabetic retinopathy. Unlike the connection between taurine and feline retinal disruptions, however, this claim remains hypothetical.

Nevertheless, it also reveals how taurine research among mammals can also influence directions regarding human-specific research.

VII. Other actions of taurine

Taurine has been suggested to be essential for prevention of depression, cirrhosis, and infertility in men as a result of low sperm motility [53]. Also, it has a potential effect on healing of acute gastric ulcers and damaged colon cells. Taurine supplementation in cystic fibrosis enhances steatorrhea, which may be due to enhanced reabsorption of bile salts. In Alzheimer's disease, memory loss is associated with low concentrations of acetylcholine; however, administration of taurine has been reported to increase brain acetylcholine. Levels of taurine are lower in patients suffering from Gaucher disease, since the availability of taurine is an essential modifier of the function of macrophages in the liver.

VIII. The reaction of hypotaurine to taurine

While taurine has been recognized as essential in humans and other mammals, there is no pharmaceutical method involving taurine to address ongoing medical or health problems. Although the list of diseases that are impacted by taurine is quite long, the defined biochemical mechanism of action is not precise. Although previous research has discovered and classified all of the enzymes located in each step of cysteine metabolism, the specific components associated with hypotaurine transformation to taurine remains unknown. The lack of information about hypotaurine to taurine processes continues to limit our full understanding of amino acid and related processes. The intensive work from the past few decades illustrates an influx of new and contradictory information and data

regarding taurine and related issues. Most studies in the past focused on the supplementation of taurine and disease linkage roles of taurine regarding health benefits.

There are two known enzymes, CSAD and CDO, that are involved in the conversion of cysteine to hypotaurine. These two enzymes and their reactions have been well studied. There is a lack of study regarding the step that involves the conversion of hypotaurine to taurine. Some analysts contend that this reaction occurs spontaneously with no enzymes involved [3]. However, one could postulate that the reaction requires an enzyme. The focus of this thesis was to study the reaction as well as to identify the enzyme and gene that are related to the biosynthesis of taurine.

IX. Figures

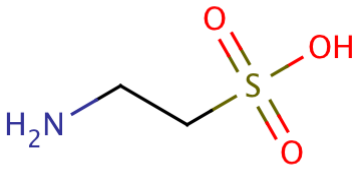

Figure 1.1. Chemical structure of taurine, which contains a primary amine and a sulfonic acid.

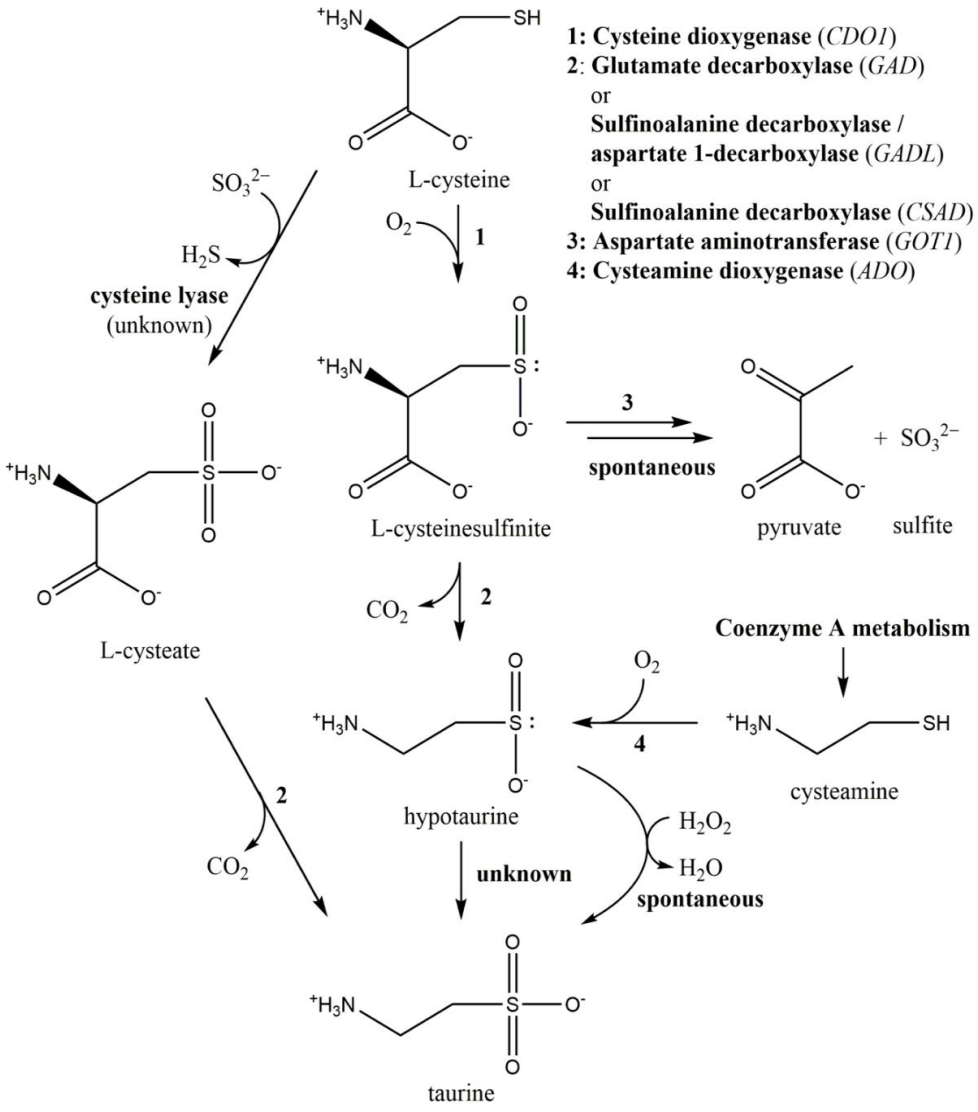

Figure 1.2. Biosynthesis pathway of taurine and list of the enzymes involved.

Chapter 2

Identifying the enzyme catalyzing the reaction of hypotaurine to taurine

I. Introduction

The awareness of taurine as a specific chemical byproduct dates back to its discovery in the early 19^{th} century [2]. In mammalian tissues, there are two main biosynthesis pathways of taurine. Taurine is formed from cysteine *via* cysteine sulfinic acid and hypotaurine intermediates [4] or from pantetheine *via* cysteamine and hypotaurine [54]. The factors resulting in the transformation of hypotaurine into taurine remains unknown and uncertain (Figure 2.1).

Sumizu [55] claimed the reaction was enzymatic. The presence of hypotaurine dehydrogenase enzyme in rat liver homogenates was detected by using the oxidation of hypotaurine with NAD^+. Flori and Costa [56] were unable to replicate the results and suggested that hypotaurine is oxidized by the trace amount of hydrogen peroxide (H_2O_2) produced by cellular metabolism. Oja *et al*. [57] used a different method and detected hypotaurine oxidation in the retinal subcellular fractions. Di Giorgia *et al*. [58] and Oja and Kontro [59] were unable to repeat Sumizu's experiment even with more sensitive methods. Oja and Kontro [59] used a radioactivity method that detected 1000X less hypotaurine oxidation than did Di Giorgia *et al*. [58] in rat liver and brain. They also could not adequately fractionate the supposed protein and suggested the protein was denaturing but had no evidence to support this explanation. Although there was no convincing evidence to prove the existence of hypotaurine dehydrogenase enzyme, many publications had claimed and misused the term hypotaurine dehydrogenase. No one has

ever isolated the enzyme and identified the protein sequence, but only the chemical reaction has been observed.

The goal of the project described in this chapter was to identify the enzyme that performs this biochemical reaction and its encoding gene (Figure 2.2). Methods included enzymatic assay and transcript co-expression analysis of known genes involved in the taurine biosynthesis pathway.

II. Materials and Methods

A. Materials

All chemical materials were purchased from Sigma Aldrich (St. Louis, MO, USA). 18.2 MΩ water from Barnstead Nanopure Ultrapure Water Purification System (Thermo Fisher Scientific, Marietta, OH, USA) was used for the preparation of aqueous solutions. A Gemini 3 μm C18 110Å 100 × 4.6 mm ID column for High Performance Liquid Chromatography was purchased from Phenomenex (Torrance, CA, USA). *Escherichia coli (E. coli*) cells were cultured. Human HuH 7 hepatoma cells were a gift from Dr. Hari Kotturi, and embryonic chicken livers were a gift from Dr. Nikki Seagraves.

B. Bioinformatics

GeneNetwork (www.genenetwork.org) [60] was searched for candidate genes that co-express with cysteine and taurine metabolism genes in human, rat, and mouse. From the co-expression list of over 100 genes, flavin-containing monooxygenase (FMO) genes showed high correlation with CSAD and CDO1 in all three organisms. Scatter plot graphs showed the tissue correlation of CDO1 and ADO with FMO1, FMO2, and FMO4.

The COXPRESdb (http://coxpresdb.jp) [61] database was searched for genes that

are co-expressed with CDO1, ADO, BAAT, and CSAD.

C. Cell lysate

Cell lysate and protein were extracted from *Escherichia coli (E. coli*) cells, human HuH 7 hepatoma cells, and 11 day-old embryonic chicken livers. Eleven day-old embryonic chicken livers had a wet weight of 0.066g to 0.099g. The cells and tissues were homogenized in 1X PBS solution by a probe sonicator (Fisher Scientific, Pittsburgh, PA, USA) with 120V 50/60Hz NOM at 120W for 10s intervals, 3 times. The homogenates were centrifuged at 15000 rpm for 5 min. The supernatants were spiked with hypotaurine and NAD^+ or NADPH, and incubated at 37°C for 4, 8, 10, and 24 hours. After the incubation period, supernatants were analyzed immediately by reverse phase HPLC.

D. High Performance Liquid Chromatography (HPLC)

The supernatants were filtered through a 3 ml syringe that attaches to 0.2 µm Thermo Scientific Nalgene Syringe Filter to remove proteins. The supernatants were analyzed by reverse-phase HPLC using an Agilent Technologies High Performance 1100 series instrument (Alpharetta, GA, USA), which was equipped with ChemStation software. *ortho*-phthalaldehyde (OPA) with 2-mercaptoethanol was used as a colorimetric tagging agent. Samples were separated by a Gemini 3µm C18 110Å 100 × 4.6 mm column. The separation was carried out by gradient elution at a flow rate of 1.2 ml/min. The elution mixture consisted of 70% of a solution of 0.1 M Na_2HPO_4 and 0.1 mM Na_2-EDTA (pH 6.38) and 30% of methanol. The emission detector was set at 360 nm.

Samples and reagents were prepared fresh for every analysis. Samples were mixed in a 1:1 dilution with the *ortho*-phthalaldehyde (OPA) reagent for 1 min before injection. The baseline for the standard curve was set up for 10 mM, 1 mM, 100 µM, 10 µM, and 1µM of hypotaurine and taurine. Before reaction with OPA, 1 M Glycine was added to the samples for use as an internal standard.

III. Results and Discussion

Results from the GeneNetwork [60] database searched for human, rat, and mouse genes indicated that flavin-containing monooxygenase genes are highly correlated with CDO1, CSAD, and ADO. Tissue correlation of twenty-six samples of tissue and organ mRNAs from taurine and cysteine metabolism showed five FMO genes in humans are positively co-expressed with CDO1 (Spearman r = 0.277 - 0.675) and CSAD (r = 0.344 - 0.628) (Table 2.1). Scatter plot graphs of Spearman Rank correlation of CDO1 *vs.* CSAD, CSAD *vs.* FMO1, FMO1 *vs.* CDO1, CDO1 *vs.* FMO2, and CDO1 *vs.* FMO4, all showed high coexpression in the liver (Figures 2.3 to 2.7).

A COXPRESdb database search confirmed the Spearman Rank correlation scatter plots graphs that CDO1, CSAD, and FMOs were highly expressed in the liver of three organisms: human, rat, and mouse. FMO is abundant in human fetal liver and is down-regulated upon birth, which corresponds to the decreasing of taurine concentration after birth. FMOs belong to the cytochrome p450 superfamily and contain a heme cofactor. FMOs are microsomal enzymes that catalyze the NADPH-dependent oxygenation and oxidation of soft nucleophiles such as sulfur and nitrogen [62]. The oxidation reaction of FMO requires a NADPH cofactor. The chemical properties found in FMO proteins would seem to be amenable to catalyzing the reaction of hypotaurine to taurine. To assist with

the FMO activities, NAD^+ and NADPH were added to cell lysate to assist the reaction of hypotaurine to taurine.

Bacteria have no hypotaurine or taurine synthesis pathway and will not demonstrate an enzymatic reaction. Hence, cell lysate from cultured *E. coli* cells was used as the negative control as it should not produce taurine after adding hypotaurine and no taurine peak should be detected from HPLC assays. HPLC assays were performed from the homogenate cell lysates from human HuH 7 hepatoma cells and eleven days-old embryonic chicken livers. The whole livers and the homogenated cell lysates were incubated with hypotaurine at 37°C for 4, 8, 10, and 24 hours to allow more products to accumulate. NAD^+ and NADPH were added to the liver and the cell lysates and incubated at 37°C for 4, 8, 10, and 24 hours to observe if a cofactor was involved in the reaction.

HPLC analysis of chemical standards showed glycine eluted at around 8 min, taurine at 12.5 min and hypotaurine at 14 min (Figure 2.8). For the *E. coli* reaction, there was no decrease in the hypotaurine peaks and no taurine peaks present. Human HuH 7 hepatoma cells and eleven days-old embryonic chicken livers showed no increase in the taurine peaks after incubation times, which suggested no chemical reaction occurred.

The results contradicted previous literature that observed the reaction of hypotaurine to taurine from liver cell lysate [55, 59]. The results also suggested the previous studies results may have observed non-enzymatic reactions. The results of this experiment did not clearly show a chemical reaction of hypotaurine to taurine. Perhaps, the cofactors used in this analysis were not compatible with the enzyme, the enzyme was inactive in the cell lysates, or the concentration of the enzyme was too low and could not

be detected within the limits of the assay procedures used.

IV. Figure and tables

Spearman Rank Correlation (rho)													
Pearson r	Gene Symbol	Fmo1	Fmo2	Fmo3	Fmo4	Fmo5	Cth	Got1	Cdo1	Csad	Gad1	Gad2	Baat	Ggt6
	Fmo1	1	0.531	0.404	0.493	0.342	0.084	0.191	0.675	0,628	-0.169	-0.195	0.159	-0.165
	Fmo2	0.662	1	0.413	0.460	0.379	0.079	0.141	0.556	0.444	0.076	-0.216	0.345	0.092
	Fmo3	0.518	0.760	1	0.338	0.415	0.236	-0.111	0.492	0.495	0.162	-0.420	-0.049	0.009
	Fmo4	0.385	0.326	0.178	1	0.599	0.310	0.171	0.508	0.354	-0.121	0.109	0.521	0.155
	Fmo5	0.318	0.217	0.096	0.555	1	0.238	0.121	0.277	0.344	-0.264	0.120	0.485	0.223
	Cth	0.307	0.047	-0.029	0.675	0.555	1	0.189	0.185	0.363	-0.047	0.186	0.311	0.570
	Got1	0.114	-0.099	-0.175	0.149	0.066	0.168	1	-0.060	-0.017	-0.181	0.157	0.246	0.361
	Cdo1	0.716	0.467	0.438	0.360	0.252	0.426	-0.176	1	0.804	0.184	-0.048	0.219	-0.200
	Csad	0.717	0.343	0.205	0.406	0.460	0.607	-0.028	0.778	1	-0.071	-0.129	0.162	0.034
	Gad1	-0.221	-0.143	-0.102	-0.247	-0.307	-0.159	0.204	-0.078	-0.183	1	0.105	0.026	-0.251
	Gad2	-0.215	-0.176	-0.187	-0.164	-0.226	-0.122	0.298	-0.100	-0.179	0.944	1	0.267	-0.046
	Baat	0.339	0.067	-0.031	0.548	0.536	0.760	0.290	0.439	0.491	-0.123	-0.074	1	0.308
	Ggt6	-0.064	0.030	-0.191	0.308	0.308	0.521	0.250	-0.120	0.159	-0.214	-0.125	0.363	1

Table 2.1. Tissue correlated results from GeneNetwork database of mRNA across 26 samples of tissues and organs for taurine and cysteine metabolism. Lower left cells list Pearson r values and upper right cells list Spearman rho values

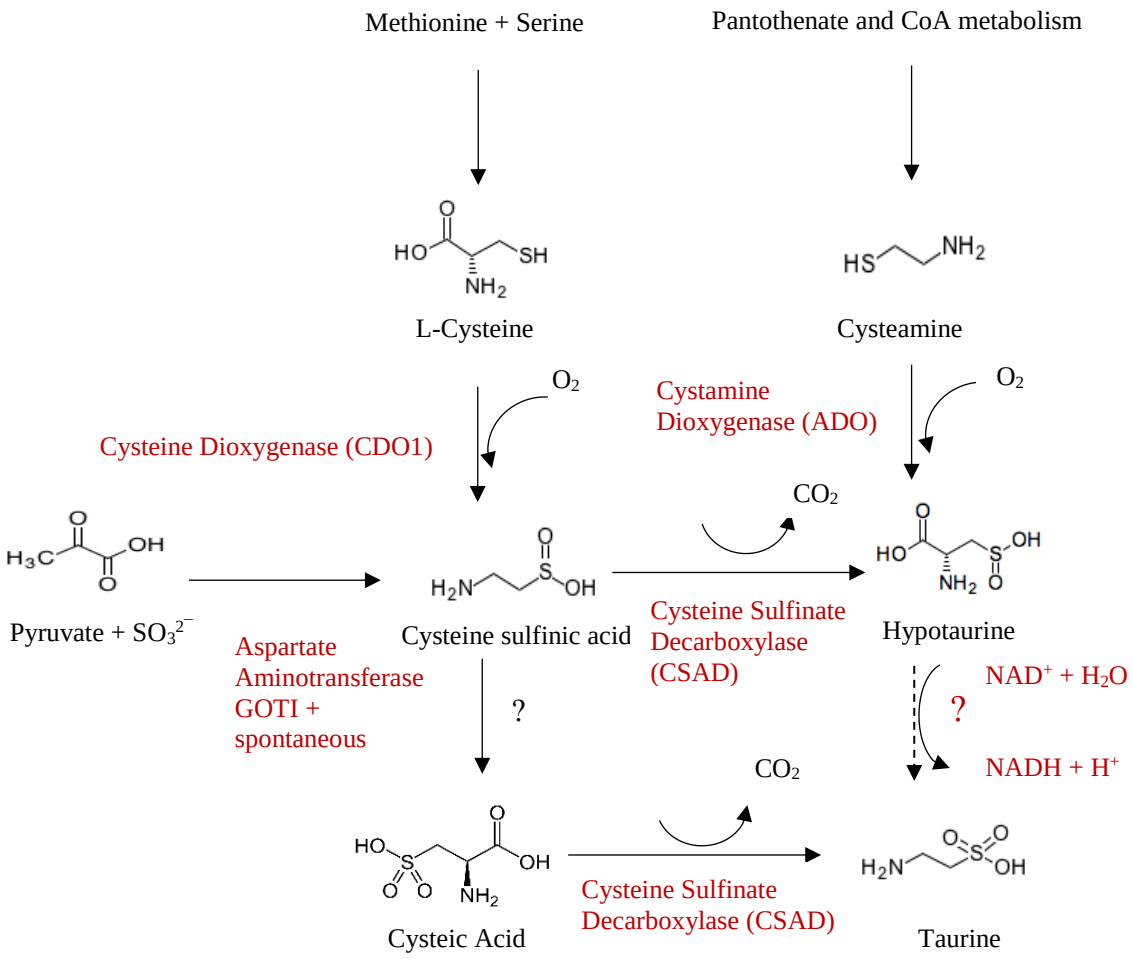

Figure 2.1. Biosynthesis pathway of taurine. L-cysteine oxidizes to cysteine sulfinic acid by enzyme cysteine dioxygenase (CDO1). Cysteine sulfinic acid then decarboxylates by enzyme cysteine sulfonate decarboxylase (CSAD) to form hypotaurine. Cysteamine oxidizes to hypotaurine by enzyme cystamine dioxygenase (ADO). The conversion of hypotaurine to taurine is still unknown.

A.

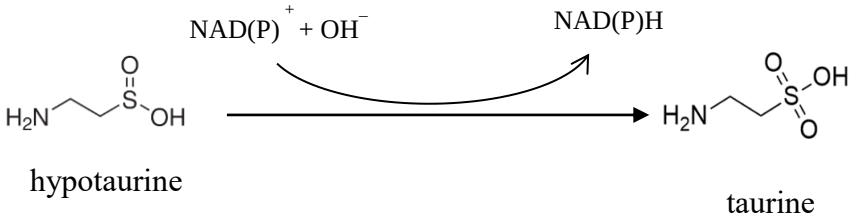

B.

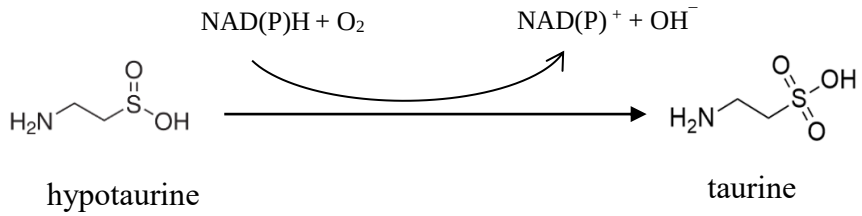

Figure 2.2. Two hypothetical enzymatic reactions of hypotaurine to taurine with co-factors (A) $NAD(P)^+$ and (B) NAD(P)H.

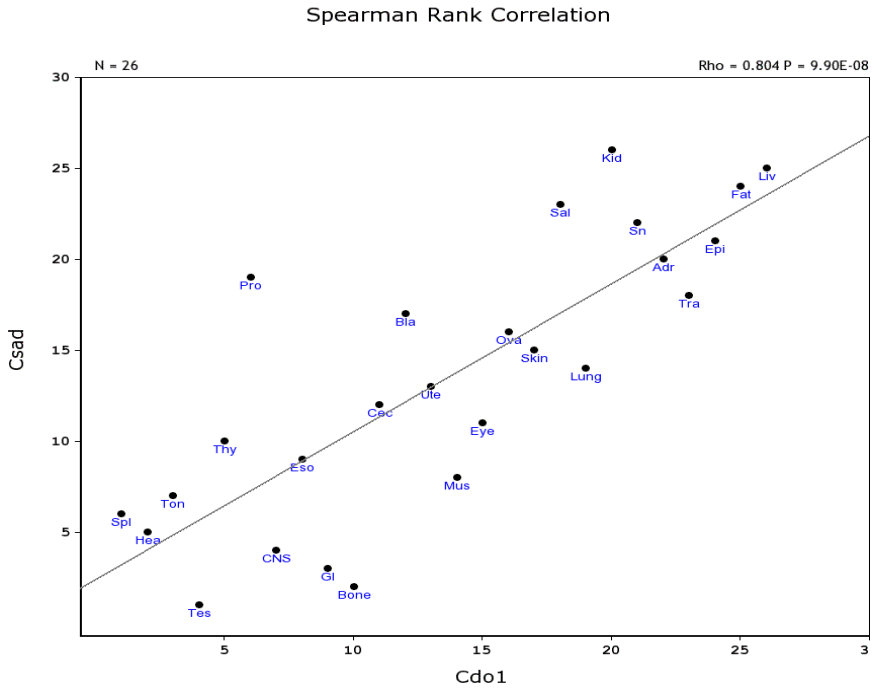

Figure 2.3. Tissue correlation scatter plot displays the correlation between CDO1 and CSAD gene.

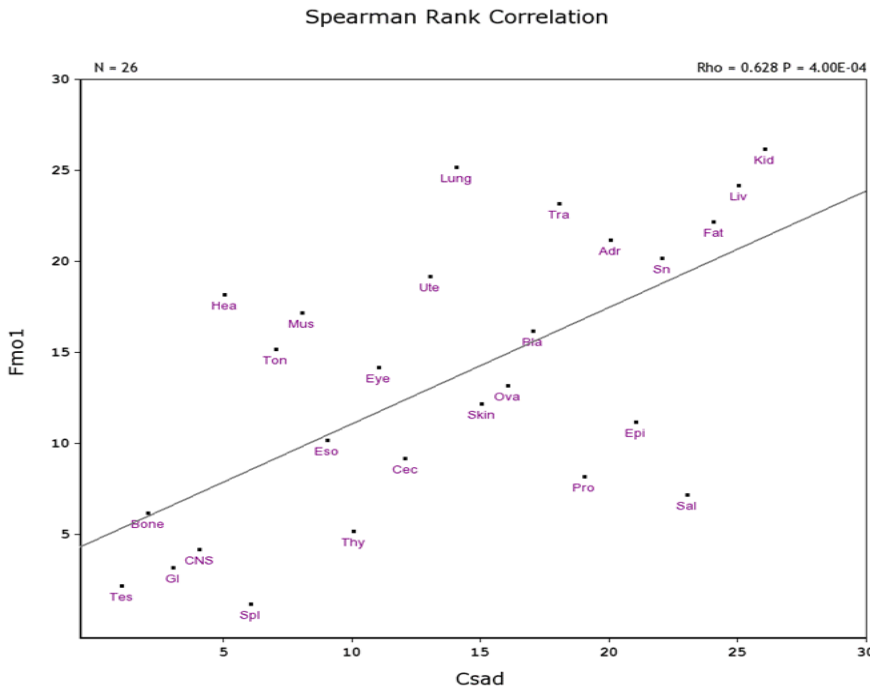

Figure 2.4. Tissue correlation scatter plot displays the correlation between CSAD and FMO1 genes.

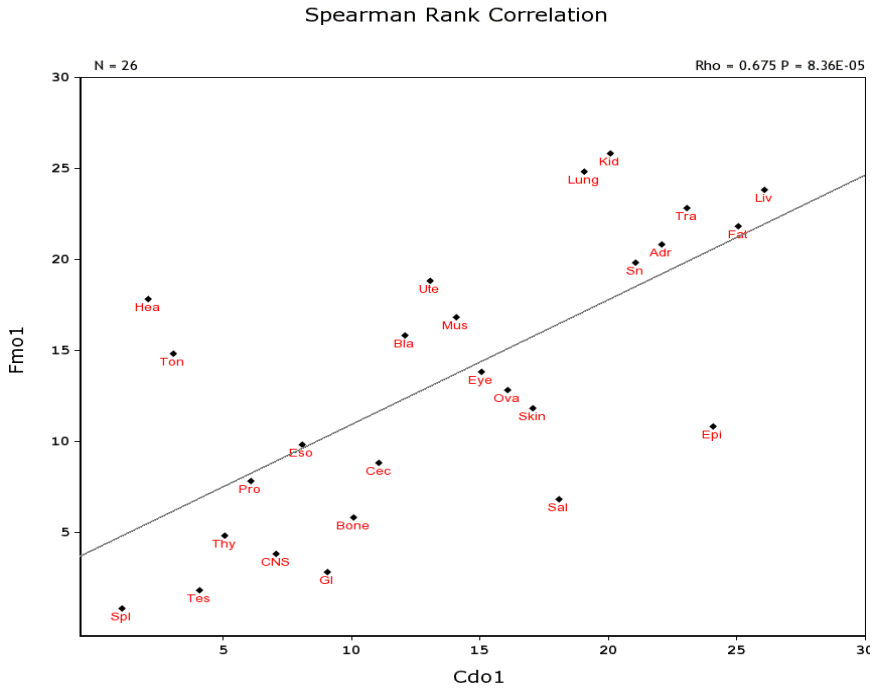

Figure 2.5. Tissue correlation scatter plot displays the correlation between CDO1 and FMO1 genes.

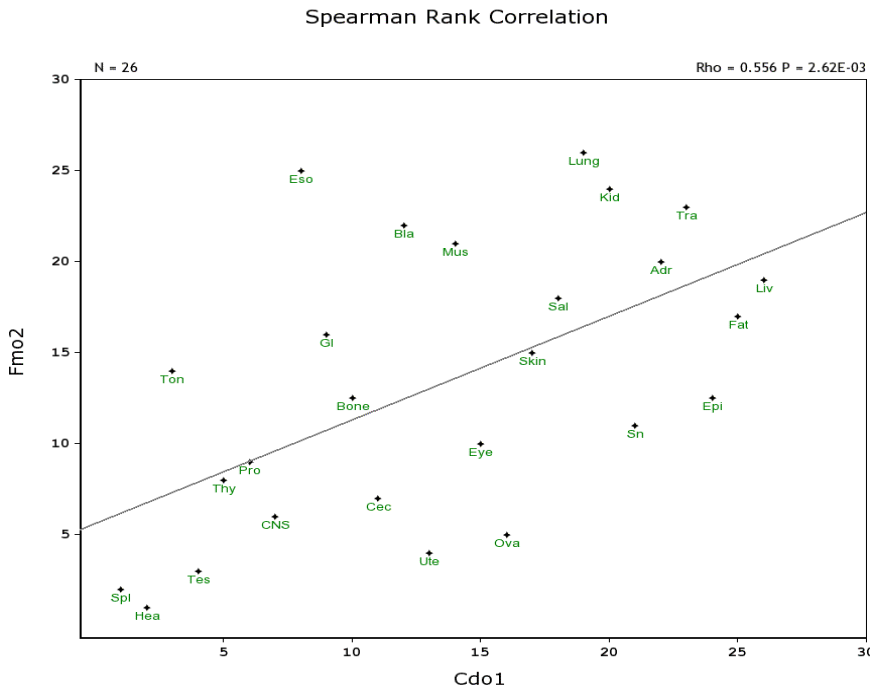

Figure 2.6. Tissue correlation scatter plot displays the correlation between CDO1 and FMO2 genes.

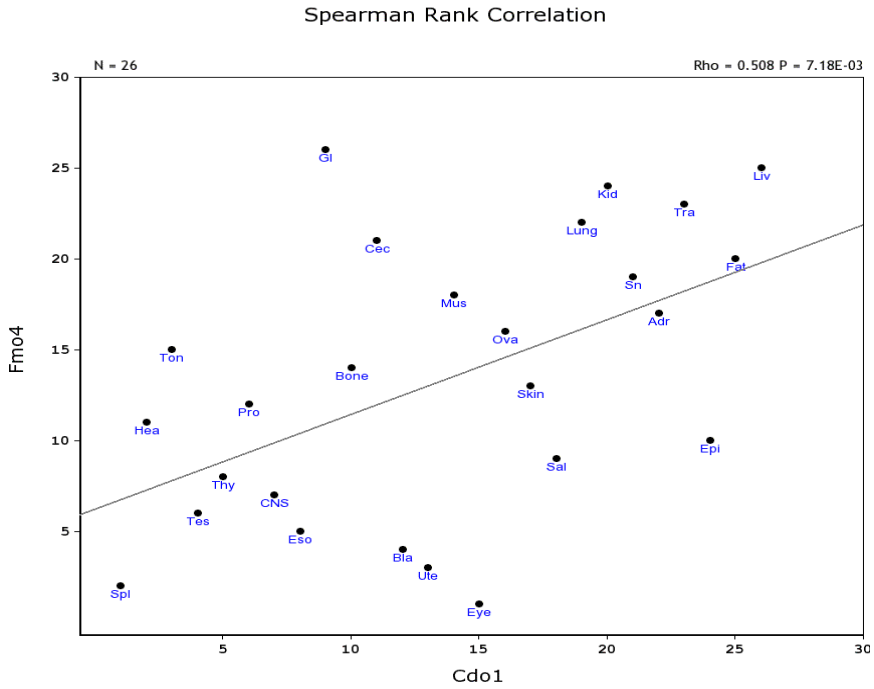

Figure 2.7. Tissue correlation scatter plot displays the correlation between CDO1 and FMO4 genes.

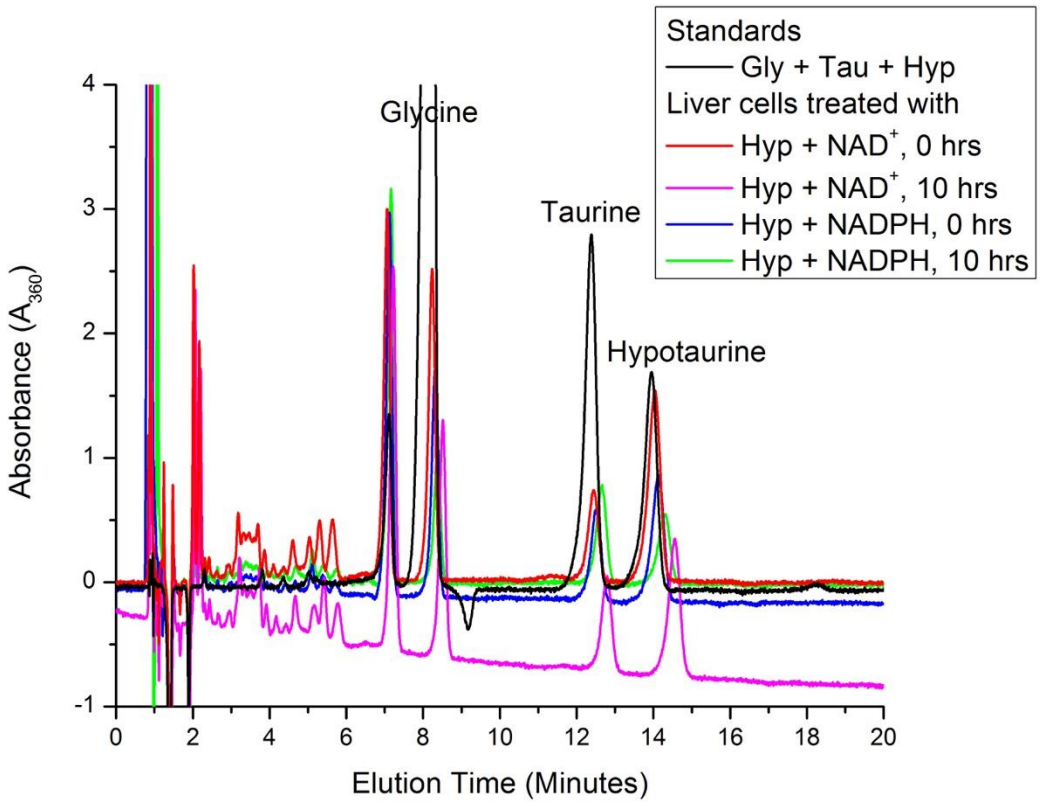

Figure 2.8. High Performance Liquid Chromatography shows the elution of taurine and hypotaurine. 1 M in cell lysate. Glycine was added to the supernatant as an internal standard immediately before sample injection. Amine-containing molecules were labeled with *o*-phthalaldehyde and detected by light absorbance at 360mm.

Chapter 3

Reaction of hypotaurine or taurine with superoxide produces the organic peroxysulfonic acid peroxytaurine

I. Introduction

Taurine is one of the most abundant, free, amino acid-derived molecules in the cells of humans and other eukaryotes. A derivative of cysteine, taurine (2-aminoethanesulfonic acid) comprises up to 0.1% of the body weight of humans [3]. It has been implicated in a number of biological processes, such as regulation of osmolality, calcium modulation, membrane stabilization, reproduction, pathogen immunity, function of the central nervous system, and neonatal development [3, 14]. Its concentration has been measured between 1 and 50 mM in liver, retina, leukocytes, neutrophils, the central nervous system, skeletal and cardiac muscles, and semen [3, 63]. Only a few biological roles for taurine are currently well understood, such as in bile acid production [3].

Along with its biological roles being poorly understood, taurine as a molecule is often mischaracterized in the scientific literature. First, it is widely called an amino acid, though it lacks the carboxylic acid that would permit that designation. Second, it is referred to as an antioxidant and has been tested for antioxidant properties in a number of studies [45, 49]. According to one study, taurine does not react readily with superoxide, hydrogen peroxide, or hydroxyl radical [45], which are some of the molecules collectively called Reactive Oxygen Species (ROS). Taurine does react with hypochlorous acid to become taurine chloramine [45], but with a rate constant 100-fold less than for the reaction of glutathione with hypochlorous acid [64]. The taurine chloramine reaction is relevant in activated neutrophils that produce hypochlorous acid,

but taurine chloramine is itself a reactive oxidizing agent [45].

Taurine is derived from the metabolic pathways of cysteine degradation and pantothenate synthesis. Cysteine is enzymatically oxidized to cysteinesulfinic acid [65], which is then enzymatically decarboxylated to hypotaurine [66, 67]. Similarly, the production of pantothenate from pantetheine produces cystamine as a byproduct. Cystamine is enzymatically oxidized to form hypotaurine [68].

The reaction of hypotaurine to taurine has been investigated but has not been clearly defined. Some early studies suggested an enzymatic conversion of hypotaurine to taurine [55, 58] but these results apparently were non-reproducible or could only measure taurine production at the detection limit [58, 59]. The identity of the putative "hypotaurine dehydrogenase" has never been clarified, but the enzymatic name has been referenced in the literature for decades as if it is a known enzyme [69, 70].

The lack of identification of an enzyme and its corresponding gene is highly problematic if one attempts to understand the apparently complex roles and regulation of hypotaurine and taurine in cells. As such, the synthesis of taurine from hypotaurine often is assumed implicitly by the literature that seeks to study taurine metabolism. If the synthesis of taurine from hypotaurine is not enzymatic, then it may be a spontaneous reaction in vivo. Interestingly, hypotaurine does appear to be an antioxidant. It reacts with hydroxyl radical, hypochlorous acid, and other oxidants with rate constants 100–10,000 times that of taurine [45, 71, 72]. Indeed, the reaction of hypotaurine with hydroxyl radical generates taurine in vitro [63]. In this study, the reactions of hypotaurine and taurine with hydrogen peroxide and superoxide have been revisited. By applying the

logic of chemical reaction mechanisms (Scheme 3.1 and Figure 3.1), the reaction of superoxide with hypotaurine would not appear to produce taurine directly, but rather through multiple reactions. Specifically, an intermediate molecule that contained a peroxysulfonic acid was hypothesized to be generated in the production of taurine from the reaction of hypotaurine with certain ROS. Here, the identity of peroxytaurine (2-aminoethaneperoxysulfonic acid) has been demonstrated *in vitro* as a semi-stable product of the reaction of superoxide with hypotaurine, and also, surprisingly, taurine. Peroxytaurine was also observed to degrade to taurine in the presence of water.

II. Materials and methods

Most chemicals, as well as XploSens PS strips, were purchased from Sigma-Aldrich (St. Louis, MO, USA). IR-grade KBr was purchased from Fisher Scientific (Pittsburgh, PA, USA). 18.2MΩ water from a Barnstead Nanopure Ultrapure Water Purification System (Thermo Fisher Scientific, Marietta, OH, USA) was used for the preparation of aqueous solutions. A Gemini 3 μm C18 110 Å 100 × 4.6 mm ID column for High Performance Liquid Chromatography was purchased from Phenomenex (Torrance, CA, USA).

A. Reactions

Standard hypotaurine and taurine solutions were prepared at 120 mM. For reactions involving hydrogen peroxide, a mixture of aqueous solutions produced final concentrations of 100 mM hypotaurine or taurine, 20 mM H_2O_2, and 40 mM Na_2HPO_4 buffer, pH 7. For reactions involving potassium superoxide, 0.005g (70 micromoles) of KO_2 was dissolved in 200 μl of a 120 mM solution (24 micromoles) of hypotaurine or

taurine. After the superoxide reaction was complete, solution pH was adjusted to 7 using 1 N HCl. The pH-adjusted reaction product solution was used for High-Performance Liquid Chromatography and Mass Spectrometry experiments. Alternatively, the pH-adjusted reaction solution was desiccated to a solid powder in an Eppendorf Vacufuge Plus vacuum centrifuge (Westbury, NY, USA). The desiccated powder was used for Nuclear Magnetic Resonance Spectrometry, Fourier Transform Infrared Spectroscopy, and Raman spectroscopy experiments. Reactions were performed fresh each day for analytical analysis.

B. Desiccated mass determination

Solutions of hypotaurine and taurine at 100, 75, 50, and 25 mM were prepared. As a control, KO_2 pellets of a mass that provided 1, 2, 3, and 4 times the molar equivalent of each of the four concentrations of reactant were dissolved in 1ml pure water. The solutions were desiccated by heating at 50°C and weighed in a weigh boat using a Denver Instrument Pinnacle Analytical balance (Bohemia, NY, USA). The measured mass was assumed to be the mass of solid potassium hydroxide plus unaccounted-for excess mass (Figure 3.2A). The excess mass was used as a correction factor in later calculations. As another control, pure water was desiccated by heat, and the difference in mass of the weigh boat before and after desiccation was used to correct for systemic error in the balance.

For the experiment proper, KO_2 pellets of the various masses were dissolved in solutions of hypotaurine or taurine at the four concentrations. The solutions were desiccated by 50°C heat then the residual mass was measured. All measurements were

conducted in experimental triplicate or more. For each of the four molar equivalent values of KO_2, a best fit line was constructed using the mass results from the 100, 75, 50, and 25 mM reaction solutions containing the same molar equivalence of KO_2 (Figures 3.2B, 3.2C). Values derived from standard curves fitted to the desiccated mass data points (Figures 3.2A - C) were used for purposes of calculating the percentage of product made in the reaction. These values were preferable compared to mean mass values at each of the four tested KO_2 concentrations because they mitigated error inherent in measuring milligram-level quantities of reagent and product.

The maximum expected values of the desiccated mass were calculated as follows: mass of peroxytaurine resulting from 100% conversion of the moles of hypotaurine or taurine reactants, plus potassium bound to reactant or product, plus remaining mass of potassium in the form of potassium hydroxide, plus the excess mass determined from the KO_2 in water control, minus the systemic error in the analytical balance. The minimum expected mass values were calculated as above except assuming all of the hypotaurine and taurine reactants remained in solution. A comparison of the product mass, as determined from the best fit line, to the maximum and minimum expected masses, produced a percentile that was interpreted as an approximate representation of reaction completion.

Measurement of the mass of degrading peroxytaurine was performed by exposing 1 ml of a 100 mM solution of taurine to 4 molar equivalents potassium superoxide. The pH of the solution was adjusted to 7 using 1 N HCl, and 1 µl of 10000 Units catalase was added to the solution. Solutions were stored at 24°C for up to 3 days. At time points of 0,

1, 2, and 3 days, solutions were desiccated by heating at 50°C, and the residual mass was measured. The control substituted pure water in place of taurine solution.

C. High Performance Liquid Chromatography (HPLC)

HPLC analyses were performed using an Agilent Technologies High Performance 1100 series instrument (Alpharetta, GA, USA), which was equipped with ChemStation software. Since hypotaurine and taurine do not absorb visible light, *ortho*-phthalaldehyde (OPA) with 2-mercaptoethanol was used as a colorimetric tagging agent. Prior to reaction with OPA, 1 M glycine was added to the sample to a final concentration of 100 mM for use as an internal standard in the HPLC traces. 2.5 μl of a sample solution was auto-injected, mixed with 2.5 μl of OPA solution, and permitted to react for 1 min prior to injection into the column. The samples were separated by a 100 × 4.6 mm Gemini C18 reverse phase column. The separation was carried out with a flow rate of 1.2 ml/min and an elution mixture comprising 70% of a solution of 0.1 M Na_2HPO_4 and 0.1 mM Na_2-EDTA (pH 6.38) and 30% of methanol. OPA-tagged molecules were detected by absorbance at 360 nm.

D. Electrospray Ionization Mass Spectrometry (ESI-MS)

ESI-MS was performed on an Applied Biosciences QSTAR Elite hybrid quadrupole/Time Of Flight mass spectrometer system (Foster City, CA, USA), equipped with a NanoSpray Ion source with Borosilicate Emitters IonSpray Voltage of 1300 V. The samples were analyzed under positive ESI conditions. Analyst QS 2.0 software, using default system parameters, was used to run the instrument. Full scan mass spectra were recorded over the mass range of m/z 50–500 using time-of-fight mode. Nitrogen

was used as the curtain and collision gas. The collision energies were between 10 and 25eV. All spectra reported were averages of 50–200 scans. Superoxide reaction solutions were pH- adjusted using 1 N HCl prior to sample injection.

E. Nuclear Magnetic Resonance Spectrometry (NMR)

Solid hypotaurine, taurine and, desiccated peroxytaurine samples were dissolved in D_2O. 600 µl of the samples were transferred into a 5 mm NMR probe head. ^{1}H NMR spectra were recorded on a Varian 500 MHz NMR spectrometer at 24°C. Default system parameters were used to run the instrument.

F. Fourier Transform Infrared Spectroscopy (FTIR)

Potassium bromide discs for FTIR were analyzed on a Nicolet 6700 spectrometer (Thermo Scientific, Waltham, MA, USA) with the DTGS KBr detector plugin. Samples to be investigated were desiccated in an Eppendorf Vacufuge Plus vacuum centrifuge for 4 h before mixing with KBr powder. One mg of a desiccated sample was mixed with 1g of KBr in a mortar and pestle. The mixture was compressed to a disc in a hydraulic press under 13 t pressure for 3 min. All spectra were produced from an average of 50 scans obtained at room temperature for the range of 7400–400 cm^{-1} with an optical resolution of 1.9 cm^{-1}. Peaks were interpreted by comparison to reference tables in a handbook [73] by analysis using IRanalyze software (LabCognition Analytical Software, Cologne, Germany), and by de novo prediction by General Atomic and Molecular Electronic Structure System (GAMESS) software [74, 75].

G. Raman spectrospray

Raman spectra were observed on a DeltaNu Advantage 200A Raman spectrometer (Laramie, WY, USA). Commercial hypotaurine and taurine crystals were used as control samples. Desiccated peroxytaurine reaction product retains water, which interfered with measurements. Thus, solid peroxytaurine-potassium bromide discs produced for FTIR, as described above, were used as samples. All spectra were produced from an average of 5 scans with an integration time of 10 s. Spectra were obtained at room temperature using the high-resolution mode (3.125 cm^{-1} resolution) over the spectral range 3400–200 cm^{-1}. Peaks were interpreted by comparison to reference tables in a handbook [73], by analysis using RAMalyze software (LabCognition Analytical Software, Cologne, Germany), and by de novo prediction by GAMESS software [74, 75].

H. Isotope labeling

Isotopic hydrogen peroxide ($H_2{}^{18}O_2$) enriched to > 90% (Berry & Associates, Dexter, MI, USA) at a concentration of ~500 mM was reacted with an equimolar volume of 100 mM hypotaurine in a 240 µl reaction. The solution was permitted to react for 2 h at room temperature and then was desiccated by 50°C heat to form a crystal. One such sample was used as a solid crystal for Raman spectroscopy via a contracted service (Moore Analytical, Houston, TX, USA). A second reaction sample was re-suspended in 200 µl water to produce a 100 mM ^{18}O-labeled taurine solution. This solution was reacted with 0.0057g (4 molar equivalents) of potassium superoxide. The reaction solution was desiccated by heat to a solid crystal and used for Raman spectroscopy via contracted service.

I. Hydrogen peroxide assay

Solutions of taurine at 25mM were reacted with 1–4 molar equivalents of potassium superoxide. The pH of the product solution was adjusted to below 7 using 1 N HCl in order to eliminate HOO^- ion, which is abundant at pH 12 and has a larger extinction coefficient than HOOH. Samples were then diluted up to 10-fold in water. The solutions were analyzed by a UV/Vis Spectrophotometer (Varian Cary 50 Bio, Agilent Technologies, Santa Clara, CA, USA) in the range of 200–500 nm. Absorbance values at the wavelength of 250 nm were selected for data analysis. As a control, potassium superoxide was reacted in water alone. A standard solution of hydrogen peroxide also was diluted to various concentrations and measured. One-way t-tests were performed for statistical analysis.

III. Results and discussion

A. Hydrogen peroxide reactions

The reactions of hypotaurine and taurine with hydrogen peroxide were investigated. A 200 μl, a phosphate-buffered aqueous solution of 100 mM hypotaurine, pH 7, was reacted with 20 mM of hydrogen peroxide. The reaction was performed both with and without 1.25 mM of the chelator diethylenetriaminepentaacetic acid (DTPA). Samples were permitted 20 min to react. High-performance liquid chromatography (HPLC) (Figure 3.3) and electrospray ionization-mass spectrometry (Figure 3.5C) of the reaction solutions were performed to evaluate the product molecules. When compared to phosphate-buffered hypotaurine and taurine standards (Figures 3.3, 3.5A, 3.5B), the H_2O_2 reaction revealed that taurine was produced from hypotaurine. Addition of DTPA did not

affect the appearance of a taurine peak in HPLC traces of the hypotaurine reaction (Figure 3.4). The evidence suggests that taurine was formed from a direct reaction of hypotaurine with hydrogen peroxide (Scheme 3.1 and Figure 3.1). The taurine product does not appear to result from the reaction of hypotaurine with hydroxyl radicals arising from metal-catalyzed hydrogen peroxide cleavage.

The result of the hypotaurine reaction agrees with a previous study that observed a reaction between hypotaurine and hydrogen peroxide using HPLC methods [63], but disagrees with another study that did not observe a reaction of hydrogen peroxide with hypotaurine [45]. This discrepancy may be due to the latter study using a peroxidase-based colorimetric assay to detect changes in hydrogen peroxide concentrations indirectly, while the former and present study detected the product taurine directly using analytical techniques. As described below for the isotope labeling experiment, an equimolar mixture of hypotaurine and hydrogen peroxide yielded complete conversion to taurine within two hours, suggesting the reaction's rate constant is not insignificant. As with hypotaurine, a buffered aqueous solution of 100mM taurine, pH 7, was reacted with 20 mM of hydrogen peroxide. HPLC and mass spectrometry revealed no large molecules in the reaction mixture other than taurine (Figures 3.3, 3.5D), which indicated taurine does not react with H_2O_2.

B. Superoxide reactions

The reactions of hypotaurine and taurine with superoxide were investigated. An unbuffered, 200 µl aqueous solution of 120 mM hypotaurine (24 micromoles), pH ~5, was reacted with 3 molar equivalents (70 micromoles) of solid potassium superoxide. Unbuffered reactions were performed because the buffer concentrations attempted proved

unable to maintain the reaction's pH, and the buffer molecules would interfere with downstream analytical analyses. Upon addition of KO_2 pellets to the solution, oxygen gas bubbles and heat were produced for approximately 4 s. After completion of the reaction, the pH of the solution was ~12, which is similar to the pK_a of hydrogen peroxide at 11.8. A similar reaction also was performed using 120 mM taurine, pH ~5, in place of hypotaurine. Again, the product solution's pH was ~12.

As a side reaction in both experiments, H_2O_2 and O_2 were produced due to spontaneous dismutation of superoxide. Taurine and hypotaurine are poorly soluble in solvents other than water, so the aqueous solution that promoted the dismutation side reaction was necessary for this experiment. At a low pH, the dismutation reaction involving hydroperoxyl ($HO_2^{\bullet}$) occurs with a rate constant of $> 10^5\ M^{-1}\ s^{-1}$. As the pH would rapidly change to 12 dues to consumption of ~2 nmol H^+ by hydrogen peroxide, the dismutation reaction's rate constant for superoxide anions ($O2^{\bullet-}$) approaches $0.3\ M^{-1}\ s^{-1}$ [76]. Therefore, most of the superoxide anions would react with hypotaurine or taurine. The results are shown in Figure 3.5E and the NMR experimental results presented below reveal that the hydrogen peroxide generated as a side product did not noticeably compete with the superoxide for reaction with hypotaurine during the few seconds before reaction completion.

HPLC analysis of the products of the reaction of hypotaurine or taurine with potassium superoxide revealed peaks with elution times equivalent to the taurine standard (Figure 3.3). The chemical identity of the peaks' components was investigated subsequently with additional analytical techniques.

For other downstream experiments, the product of the superoxide reaction was dried to a white powder using a vacuum desiccator to remove water and hydrogen peroxide. The powder, as a potassium salt, exhibited hygroscopic and electrostatic properties. Most subsequent analyses used either the desiccated powder or a solution in which the powder was re-suspended with ultrapure water.

In HPLC analysis, the product reacted at pH 7 with *ortho*-phthalaldehyde (OPA), a colorimetric tag that reacts with primary amines. Thus, the primary amine in hypotaurine and taurine was not oxidized by superoxide. Oxidation of the amines was not logically expected to occur as a chemical reaction anyway. Additionally, OPA-tagged product eluted at the same time and is indistinguishable from OPA-tagged taurine (Figure 3.3). This result suggested a reason why the product molecule (peroxytaurine) has not been previously observed in investigations of hypotaurine reactions or taurine metabolism, which have relied primarily upon chromatographic methodologies. For the HPLC experiment, only 2 molar equivalents of KO_2 were exposed to hypotaurine or taurine to achieve incomplete conversion, so that both reactant and product molecules would be visible on the HPLC trace.

C. Mass spectrometry

To determine the number and masses of products generated by the superoxide reaction, electrospray ionization-mass spectrometry (ESI- MS) was performed. A reaction solution (pH~7) of hypotaurine and superoxide revealed three unknown peaks at a mass-to-charge ratio (m/z) of 112.9, 164.0, and 201.9 (Figure 3.5E). Taurine peaks of 126 or 148 m/z were not present. The peak at 164.0 would suggest a product molecule

corresponding to the mass of a hypotaurine (132 m/z) plus two oxygen atoms (32 m/z). Additional peaks were observed at different pH values of the product solution. For an un-adjusted reaction solution of pH~12, peaks at 94.9, 176.9, and 201.9 m/z were observed (Figure 3.6A). For a reaction solution adjusted to pH~4, peaks at 148.9, 164.0, and 201.9 m/z were present (Figure 3.6B). The true masses of hypotaurine and taurine positive ions are 110 and 126 m/z, respectively, but these are one of the multiple peaks in the hypotaurine (Figure 3.5A) and taurine (Figure 3.5B) standards observed under positive ESI conditions. Zwitterions associated with Na^+ may explain the hypotaurine (132.0 m/z), taurine (148.0 m/z), and product (164.0 m/z) peaks, while the negative ion of the product may associate with both Na^+ and K^+ (201.9 m/z). The multiple peaks in the product solutions also may correspond to various ionically-charged forms of the product molecule or its degradation products in the mass spectrometer.

ESI-MS of the reaction solution (pH~7) of taurine and superoxide (Figure 3.5F) reveals the same peaks as those seen in the hypotaurine reaction solution. The higher count intensity, and thus greater sensitivity of the instrument for this sample may explain why all of the putative ionically-charged product molecules mentioned above are detected in a single spectrum. Changing the pH of the product solution resulted in the same pattern of peaks as for the hypotaurine reaction (Figures 3.6C, D). The results indicate the same product molecule was generated by both the reaction of hypotaurine with superoxide and the reaction of taurine with superoxide. Again, the m/z of 148 for taurine plus one oxygen (16 m/z) would yield a m/z of 164. The m/z of the product initially suggests the hypothesized molecule named peroxytaurine (Scheme 3.1). Mass spectrometry indicates almost complete stoichiometric conversion of hypotaurine or

taurine to product molecule by exposure to 3 molar equivalents superoxide (Figures 3.5E, F). As mentioned above, in the reaction of hypotaurine and superoxide, taurine is not observed to be produced from the competing reaction of hypotaurine with the low concentration by-product hydrogen peroxide (Figure 3.5E).

D. Nuclear Magnetic Resonance Spectroscopy

To determine if the chemical modification in the product molecule was located on the central carbon atoms, ^{1}H Nuclear Magnetic Resonance Spectroscopy was performed. In D_2O, both hypotaurine and taurine present triplets for their two methanediyl groups (Table 3.1 and Figure 3.7). The product molecule resulting from a reaction of hypotaurine and superoxide revealed triplets whose central peaks' chemical shift differed from that of both hypotaurine and taurine. The hydrogen atoms of the amines and the sulfur-based acids could not be observed due to hydrogen exchange with the solvent. The result indicates that hypotaurine was modified by superoxide at either its amine or sulfinic acid to a molecule similar, but not identical, to taurine. Since the HPLC results indicate that the primary amine is not oxidized, the logical conclusion is that the chemical modification by superoxide was present on the sulfur-centered moiety. This inference further suggests that the product molecule contained an SO_4 group, likely as a peroxysulfonic acid.

E. Fourier Transform Infrared Spectroscopy

To investigate the chemical structure of the product molecule, Fourier Transform Infrared Spectroscopy (FTIR) was performed to detect bond vibrations. A FTIR spectrum

of hypotaurine (Figure 3.8A) using the potassium bromide disc method reveals a strong S–O symmetric stretching peak at 999 cm^{-1}. In contrast, taurine and the product molecule peroxytaurine reveal strong S=O asymmetric stretching peaks at 1213 cm^{-1} (Figure 3.8B) and 1194 cm^{-1} (Figures 3.8C, D), respectively. It is notable that the product molecule's spectrum is similar, but not identical, to that of taurine (Table 3.4). For example, a conspicuous medium peak at 1113 cm^{-1} in the taurine spectrum is not present in the peroxytaurine spectra. Since the bonds of the sulfur-based acid in the product molecule absorb infrared light at different frequencies than hypotaurine or taurine, the results suggest that the chemical environment of the sulfur-based acid in the product molecule is also different. Specifically, taurine contains an SO_3 sulfonic acid while the product molecule contains an SO_4 peroxysulfonic acid.

Peroxytaurine generated from either hypotaurine or taurine revealed substantially equivalent spectra. However, the peroxytaurine generated from hypotaurine and presented in Figure 3.8C has a unique peak at 962cm^{-1}, while the peroxytaurine generated from taurine and presented in Figure 3.8D has a unique peak at 1722 cm^{-1}. These peaks were not always reproducible in the FTIR experiments but are reported in case of significance. These inconsistent peaks, as well as the broadened peaks overall for peroxytaurine, likely resulted from water contamination in the KBr discs.

F. Raman spectroscopy

Raman spectroscopy can better detect symmetric bond vibrations that FTIR methods cannot, such as the stretching of O–O bonds. The Raman spectra of

peroxytaurine emphasized three strong peaks at 1090 cm^{-1}, 1065 cm^{-1}, and 837 cm^{-1} (Table 3.2 and Figure 3.9). A general trend in the results was a shift to larger frequencies for equivalent peaks in taurine and peroxytaurine relative to hypotaurine. The strongest peak seen from hypotaurine at 981 cm^{-1} corresponds to S=O stretching, while the strong peaks of taurine at 1065 cm^{-1} and peroxytaurine at 1065 cm^{-1} correspond to symmetric SO_2 stretching. C–S bond stretching yields the strong 765 cm^{-1} peaks in hypotaurine, medium 778 cm^{-1} peak in taurine, and a weak 815 cm^{-1} shoulder peak in peroxytaurine. A symmetric S=O/S–O sulfoxy bend is revealed in hypotaurine at 828 cm^{-1}. This symmetric bending mode is interrupted in the SO_3 environment of taurine or peroxytaurine, and, consequently, no equivalent peaks are observed in their spectra. Instead, peroxytaurine has a strong peak at 837 cm^{-1} that may correspond to symmetric O–O bond stretching. This interpretation is suggested by another study that observed peroxydisulfate O–O bonds absorbing at 858 cm^{-1} [77]. Notably, H_2O_2 does not absorb at any of the described frequencies, so these peaks cannot be attributed to residual H_2O_2 generated as a by-product of the synthesis reaction.

To confirm the presence of the O–O peak, an experiment was performed to label peroxytaurine with ^{18}O isotope. An ^{18}O–^{16}O absorbance peak would appear at a different frequency than an ^{16}O–^{16}O peak. In order to label peroxytaurine, two sequential reactions were performed. To begin, hypotaurine was reacted with an equimolar amount of ^{18}O-labeled hydrogen peroxide. FTIR spectra (not shown) suggested complete conversion of hypotaurine to taurine after a two-hour reaction. A Raman spectrum of the reaction

product indicates taurine contained the isotope, based on the shifting of the SO_2 stretch peak to 1014 cm^{-1} (Figure 3.10A). Almost all peaks for the labeled taurine and peroxytaurine described below exhibited a bathochromic shift relative to those presented in Table 3.2. The general shifting may be due to using of a different Raman spectroscope for this particular experiment. Furthermore, use of potassium salt crystals of sample, rather than of compressed KBr discs containing sample, can influence the physical bending arrangement, and hence vibrational frequencies, of the molecule in the crystalline solid. Regardless, the bathochromic shift of the isotopic SO_2 stretch peak is noticeable even after aligning the spectra of unlabeled and labeled taurine (Figure 3.10C).

A subsequent reaction of the labeled taurine with four molar equivalents of potassium superoxide produced labeled peroxytaurine. FTIR spectra (not shown) suggested complete conversion of taurine to peroxytaurine. A Raman spectrum reveals that the product was labeled, based on the SO_2 stretch peaks (1028, 969, and 961cm^{-1}; Figure 3.10A). The smaller and separate labeled peaks (969 and 961 cm^{-1}) from the main unlabeled peak (1028 cm^{-1}), relative to the single peak in taurine (1014 cm^{-1}; Figure 3.10B), suggests weak isotopic SO_2 symmetric stretch modes in peroxytaurine. To elaborate, the three oxygen atoms in taurine are in resonance and each has a bond order of 1.66, which contributes to the single observed peak. In contrast, the three sulfur-bound oxygen atoms in peroxytaurine are not in resonance and have bond orders of 1, 2, and 2, which creates a different environment for symmetric stretch modes of $^{16}O{=}S{=}^{18}O$, $^{16}O{=}S{-}^{18}O$, and $^{18}O{=}S{-}^{16}O$ relative to $^{16}O{=}S{=}^{16}O$ or $^{16}O{=}S{-}^{16}O$.

The $^{16}O–^{16}O$ stretch mode is observed at 802cm^{-1}, with an adjacent peak at 739 cm^{-1}, which suggests the $^{18}O–^{16}O$ stretch mode (Figure 3.10D). It should be noted that the frequency of the $^{18}O–^{16}O$ symmetric stretch mode is influenced by the S–^{18}O stretch modes. A simple linear harmonic oscillator model of two coupled diatomic molecules, with ^{18}O as the central atom, predicts a shift of the O–O vibrational frequency from 802 cm^{-1} to 749 cm^{-1}. The observed peak at 739 cm^{-1} does not appear to be identical to the labeled taurine peak at 730 cm^{-1} (Figure 3.10B).

Hydrogen peroxide is observed in the peroxytaurine Raman spectrum, which may be due to some of the superoxide reaction by-product being trapped in the heat-desiccated salt crystal and/or minor degradation of peroxytaurine that occurred during sample transit prior to measurement. The $^{16}O–^{16}O$ peak at 874cm^{-1} closely matches the literature value for hydrogen peroxide of 877cm^{-1}. Furthermore, isotopic hydrogen peroxide, indicating some legitimate degradation, presents an $^{18}O–^{16}O$ peak at 840 cm^{-1}, which is similar to the linear harmonic oscillator model's predicted value of 838 cm^{-1}. and a literature value of 847 cm^{-1}

G. Stoichiometry

To determine the extent of reaction completion and thus provide insight into the reaction stoichiometry, a gravitometric experiment was performed that measured the desiccated mass of peroxytaurine. Hypotaurine (109 g/mol) and taurine (125 g/mol) have less mass than peroxytaurine (141 g/mol). The mass of reaction product was compared to

that of calculated product masses, which were the minimum and maximum expected masses due to, respectively, fully un-reacted and fully reacted hypotaurine or taurine. For example, the expected maximum masses of peroxytaurine were calculated by assuming complete conversion of hypotaurine or taurine to peroxytaurine regardless of superoxide concentration, and by assuming that dry K^+ was bound to reagent and in the form of potassium hydroxide. Comparing the measured masses to the difference between the calculated maximum and minimum masses would indicate the percent conversion of hypotaurine or taurine to peroxytaurine. In the experiment, 1 ml of various concentrations of hypotaurine or taurine were reacted with between 1 and 4 molar equivalents of potassium superoxide. Samples were then desiccated by heat to dry residue. Heat desiccation of pure water and aqueous solutions of potassium superoxide served to provide control masses for calculation of expected values.

The results (Table 3.3, Figure 3.2) indicate that reactions of both 3 and 4 molar equivalents of KO_2 with hypotaurine or taurine produced final masses that are > 75% of the difference between the predicted maximum and minimum masses of the product's potassium salt mixture. The results of the FTIR, ESI-MS, and NMR experiments discussed above indicate complete or near complete conversion of hypotaurine or taurine to peroxytaurine when using > 3 molar equivalents of potassium superoxide. Thus, the reaction completion percentiles are not exact but reveal a general trend.

In the reactions involving 2 molar equivalents of KO_2, the product masses, relative to expected, are ≥15% less than that of product in the reactions with 3 molar equivalents KO_2. These results suggest incomplete conversion to peroxytaurine. By

accounting for the spontaneous dismutation of superoxide in water, which consumes an initial quantity of the superoxide, the overall experiment's results appear to support the reaction stoichiometry suggested in Scheme 1. Specifically, greater than 2 molar equivalents of superoxide were necessary in practice for reaction completion due to some loss of superoxide in side reactions.

One molar equivalent of KO_2 presented different results for taurine versus hypotaurine. While about half of the taurine appears to have consumed almost all of the superoxide to convert to peroxytaurine, less of the hypotaurine converted to product. One possible explanation is that hypotaurine engaged in both reduction and oxidation reactions with superoxide and thus served as a catalyst for its dismutation in solution. Alternatively, the rate of the hypotaurine reaction may be more dependent on superoxide concentration than in the taurine reaction. Challenges with precise measurements prevented useful experiments using less than 1 molar equivalent KO_2.

An additional experiment, involving spectroscopic measurement of produced hydrogen peroxide, was conducted to further inform reaction stoichiometry. Reactions of potassium superoxide in pure water or solutions of 25 mM hypotaurine or taurine were performed. The pH of the product solutions was adjusted to below 7 to mitigate spectroscopic absorbance by hydrogen peroxide anion. The absorbance of light at 250 nm indicated the concentration of hydrogen peroxide. The results (Figure 3.11) suggest that one hydrogen peroxide was produced per two superoxides in both the hypotaurine and taurine reactions, as well as for the dismutation of superoxide in water. There is no statistical difference between the three samples' mean absorbance values at each of the

four concentrations of KO_2 used.

The production of one hydrogen peroxide per peroxytaurine molecule was expected for the reaction of hypotaurine with superoxide. One hypothetical reaction mechanism (Figure3.1C(a)) postulates oxidation of the sulfinic acid by superoxide followed by formation of a covalent bond between the sulfinic acid radical and a second superoxide. The initial reaction step involving oxidation of hypotaurine and reduction of superoxide likely has a net unfavorable reduction potential and would be slow, which contradicts the observed rapid reaction. However, it should be noted that the reaction occurred near pH 12, which would have altered the standard reduction potentials. An alternative mechanism (Figure 3.1C(b)) involving initial nucleophilic attack of superoxide on hypotaurine and subsequent one electron transfers may not have as unfavorable reduction potentials within the transition states. Favorable thermodynamic features must compensate for any unfavorable reaction steps to yield an overall exergonic reaction, as evidenced by the release of heat. Such features may include increased entropy, decreased solvation enthalpy, and/or a negative heat of formation.

The production of just one hydrogen peroxide in the superoxide reaction with taurine was unexpected. Most potential reaction mechanisms involving the conversion of one taurine to one peroxytaurine in the presence of two superoxides suggest either zero or two hydrogen peroxide molecules produced per peroxytaurine. It is possible that multiple mechanisms are used simultaneously. However, a potential mechanism that produces a single hydrogen peroxide product involves two superoxides reacting with a single taurine to yield one hydrogen peroxide and one atomic oxygen, which would rapidly react with dioxygen to form ozone. Such a mechanism is unlikely, as spectroscopic measurements

of the head gas following reactions in a closed quartz cuvette failed to detect an ozone peak at 254 nm (data not shown). Alternatively, a mechanism involving two taurines reacting with two superoxide molecules to yield peroxytaurine, hypotaurine, hydrogen peroxide, and dioxygen is plausible. The hypothesized taurine mechanism has similarities to the hypotaurine mechanism in that there are two potential pathways (Figures 3.1D(a) and 3.1D(b)). Whether the initial reaction steps have a positive or negative reduction potential depends on the exact mechanism. Regardless of the mechanism, the overall reaction is exergonic, for similar reasons as suggested above for the hypotaurine reaction. If hypotaurine is produced as a product of the taurine reaction, it also would have reacted with superoxide in a manner consistent with the observed results.

An attempt was made to measure the rate constant of the superoxide reactions. Hypotaurine and taurine do not absorb in the visible or near- UV spectrum, but H_2O_2 production can be detected at 250nm. However, the maximum limit of detection on a UV–Vis spectrophotometer was reached within the minimum measurement interval of 12.5 ms after mixing KO_2 with the solution. These technical challenges and the rapid reaction (> 25 mM hypotaurine converted in a matter of seconds) precluded direct rate experiments based on the available equipment. A previous study has suggested the reaction rate constants of hypotaurine or taurine with superoxide are $< 10^3\ M^{-1}\ s^{-1}$ [45]. However, that study was unable to detect reactions between superoxide and hypotaurine or taurine due to using indirect cytochrome c- and Nitro Blue Tetrazolium-coupled assay systems.

H. Chemical properties of peroxytaurine

A titration curve of peroxytaurine in water at 24°C (data not shown) revealed two pK_a values that would correspond to deprotonation of the primary amine at pH 9.78 and deprotonation of the peroxysulfonic acid at pH 6.28. In comparison, the measured pK_a of taurine's amine was 9.25 (data not shown). The pK_a of taurine's sulfonic acid was inferred to be 1.51 based on a solution pH of 5.38 after dissolving crystalline taurine in water. These results were similar to published pK_a values for taurine of ~1.5 and 9.08 (Albert, 1950). The large difference in pK_a of the sulfur-based acid (6.28 versus 1.51) suggests the terminal –OH group of peroxytaurine is chemically distinct from that of taurine's sulfonic acid. The deprotonated, negatively-charged oxygen would be resonance- stabilized in taurine, thus permitting a low pK_a. As is typical of peroxy acids, the peroxysulfonate form of peroxytaurine would not be resonance-stabilized and would be less energetically favorable, hence the higher pK_a.

A chemical test for the presence of a peroxide using a commercial colorimetric peroxide detection strip (XploSens PS, Sigma-Aldrich) yielded a positive result immediately after reaction of superoxide with hypotaurine or taurine. Subsequent treatment of the solution with catalase produced gas bubbles. The solution then would yield a negative result (data not shown). Curiously, the desiccated, solid product molecule tested negative when pressed against the detection strip. Upon re-suspension of the product powder in water, the peroxide test again showed a positive result. However, treatment of the re- suspended solution with catalase followed by sampling with the detection strip would produce a negative result. Hydrogen peroxide generated by the dismutation reaction of superoxide and in the production and degradation of peroxytaurine (Scheme 3.1 and Figure 3.1) was the likely source of the positive test

result. Catalase is specific for its substrate, hydrogen peroxide. Addition of catalase removed the hydrogen peroxide and eliminated the positive test result. The peroxide test apparently was insensitive to the peroxysulfonic acid.

A solution of peroxytaurine freshly prepared from hypotaurine did not show hypotaurine or taurine signals in ESI-MS (Figure 3.5E). To clarify if peroxytaurine spontaneously degrades in water, a solution of freshly prepared peroxytaurine was adjusted to pH 7 and treated with catalase. Samples were stored at 24°C for up to three days. The pH of the solutions remained ~7 through day three, implying catalase remained functional to remove hydrogen peroxide. Results suggest that most of the peroxytaurine degraded to a final mass equivalent to taurine within three days (Figure 3.12). It was expected that the rate of degradation decreases according to exponential decay over subsequent days as the concentration of peroxytaurine is reduced. This result, as well as that of the commercial peroxide test described above, suggests that peroxytaurine degrades in water to taurine and hydrogen peroxide (Scheme 3.1 and Figure 3.1).

I. Potential biological significance

Cells produce large quantities of superoxide during normal metabolic processes. Approximately 1–3% of O_2 that encounters mitochondria is converted into superoxide anion [78] $O_2^{\bullet-}$ is poorly soluble in membranes but can diffuse more readily in the form of $HO_2^{\bullet}$. Hydroperoxyl can initiate certain lipid peroxidation events and react with existing lipid hydroperoxides to form lipid peroxyl radicals [76]. The $O_2^{\bullet-}$ or $HO_2^{\bullet}$ that is soluble in water can be removed enzymatically by superoxide dismutase to form

hydrogen peroxide. The results presented in this work suggest that superoxide can react spontaneously with hypotaurine or taurine, which can be present at micromolar or millimolar concentrations, respectively, in cells [3, 63]. It is reasonable to assume that the chemistry demonstrated in vitro would apply *in vivo*. Indeed, hypotaurine has been observed to protect against lipid peroxidation [79]. Since hypotaurine and taurine in a cell are likely maintained at steady state concentrations, the results presented herein suggest that the reaction rate of these molecules with superoxide would be dependent primarily upon superoxide concentration. Because up to 10–30% of O_2 may be converted to superoxide during exercise [78], the rate of production of peroxytaurine may greatly increase during periods of cellular exertion.

One complicating factor as to the potential abundance of peroxytaurine in cells is the reaction mechanism. The reactions to form peroxytaurine are likely multi-step (Figure 3.1). For *in vitro* experiments, two superoxide molecules were required per reagent to achieve conversion to product. In a cell, other oxidants could potentially substitute in place of one of the superoxide molecules. Depending on the reaction mechanism, some type of radical would be formed in the transition states. A previous study revealed that the sulfinyl radical of hypotaurine is an unstable intermediate, which can rapidly react with another radical in vitro [63]. In a complex biochemical system, any sulfinyl, sulfonyl, or peroxyl radical may react with biological molecules other than a superoxide or an appropriate redox-active molecule that is useful to yield peroxytaurine. Quenching of a transition state radical in vivo to restore hypotaurine or taurine may serve as a propagation mechanism for radical chain reactions. Alternatively, a transition state radical may quench with antioxidant molecules known to contain radicals, such as

ascorbate. While the reactions demonstrated herein were spontaneous in vitro, the possibility remains open that one or more enzymes may exist that catalyze reactions of hypotaurine and taurine with reactive oxygen species.

The results in this work indicate that hypotaurine can react with hydrogen peroxide to form taurine. While catalase and glutathione peroxidases are effective enzymes for the elimination of hydrogen peroxide, their localization to the mitochondria, peroxisomes, or other subcellular locations may limit their ability to remove hydrogen peroxide that is generated or diffuses elsewhere in a cell or outside a cell. Hypotaurine may serve as an antioxidant in the cytosol and in other cellular and extracellular locations where it is abundant. For example, neutrophils may contain about 120 μM hypotaurine in their cytosol, as calculated from published hypotaurine quantity [63] and cell volume [80] data. Hypotaurine may protect against oxidants such as hydrogen peroxide, which are generated by neutrophils yet can cross membranes.

Numerous studies rely on liquid chromatography methods to detect taurine [81-83]. Peroxytaurine appears to elute similarly to taurine in standard chromatographic methods used to detect amino acids and similar biological molecules. Thus, a question may be raised as to what quantity of detected biological taurine is, in fact, co-eluted peroxytaurine. Additionally, peroxytaurine can degrade to taurine and hydrogen peroxide and thus can be considered a pro-oxidant. The perception of taurine as an antioxidant, specifically against superoxide, should be reconsidered in this context.

J. Summary

Hypotaurine was observed to react to taurine in the presence of hydrogen

peroxide. Both hypotaurine and taurine react with superoxide. The product gained 32 m/z units over hypotaurine and 16 m/z units over taurine, but it runs at an equivalent elution time as taurine in HPLC. Amine-labeling of compounds for HPLC suggests no chemical modification of the primary amine in the product. No chemical modification of the two carbons in the product occurred. FTIR and Raman results suggest an altered SO_3 environment in the product, relative to taurine, with the appearance of an interpreted O–O bond vibration in the Raman spectra. The product has a higher pK than taurine's SO_3, and it degrades in water to yield hydrogen peroxide. Collectively, the results suggest an addition of two oxygen atoms to hypotaurine and one oxygen atom to taurine to form an SO_4 moiety, with the chemical evidence indicating the formation of a peroxysulfonic acid.

IV. Figures and tables

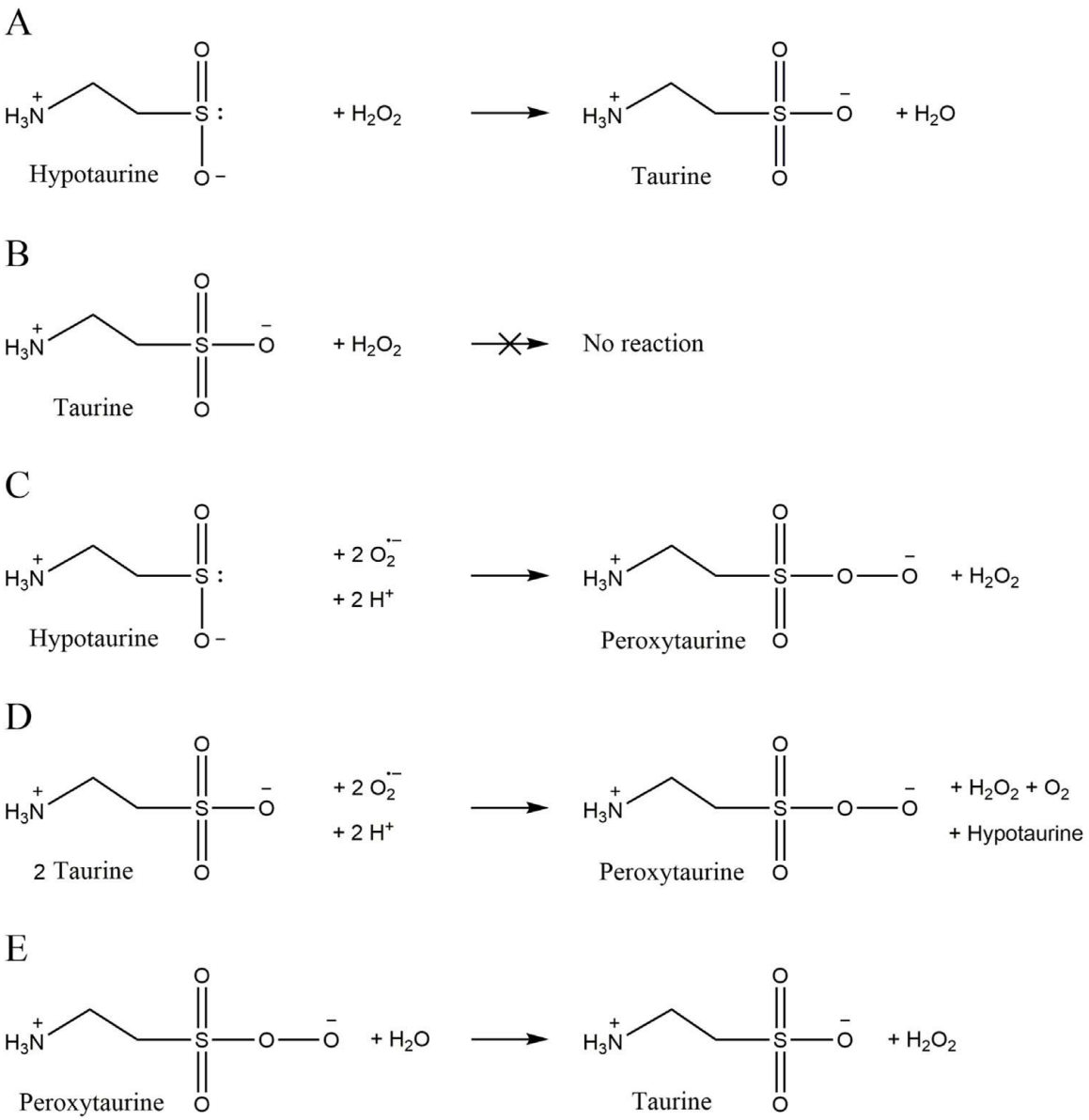

Scheme 3.1. Proposed chemical reactions involving hypotaurine and taurine. Synthesis reactions are shown involving hypotaurine (A) and taurine (B) with hydrogen peroxide or hypotaurine (C) and taurine (D) with superoxide anion. Degradation of peroxytaurine (E) is shown. A pH of 7 is assumed in presentation of the protonation state of chemical groups.

Table 3.1. The chemical shift of triplet main peak from ^{1}H-Nuclear Magnetic Resonance spectra.

	Carbon-α (ppm)	Carbon-β (ppm)
Hypotaurine	3.336	2.621
Taurine	3.409	3.242
Peroxytaurine	3.397	3.237

Table 3.2. Peaks and vibration modes from Raman Spectroscopy spectra.

Vibration mode	Hypotaurine	Taurine	Peroxytaurine
		431	412
		531	
SO_2 wag	600	581	590
		644	662
			744
C-S stretch	765	778	815
S=O/S-O sym. bend	828		
O-O stretch			837
		888	
		934	
		996	
S=O stretch	981		
SO_2 sym. stretch		1065	1065
	1018	1084	1090
			1128
CH_2 twist	1075, 1106, 1192, 1281	1140, 1209, 1285, 1369	1222, 1287
	1363, 1441	1453	1397, 1447
CH_2 scissoring	1485	1481	1490
NH_3 asym. bend	1635, 1659	1634	1619
	2878, 2943	2806, 2884, 2950	2944
NH_2 sym. stretch	2966	2994	2985
NH_2 asym. stretch	3022	3028	3009
			3378

Assigned peaks are aligned in rows with indicated vibration mode. Other unassigned peaks are listed in order of frequency (cm^{-1}) and have no particular association with other frequencies in the same row. Sym=symmetric. Asym=asymmetric.

Table 3.3. Percentile product mass in reactions with KO_2 relative to expected mass.

mol KO_2 / mol taurine or hypotaurine	1	2	3	4
Hypotaurine	12.1% (± 22.6)	70.9% (± 3.3)	87.4% (± 2.1)	84.0% (± 2.3)
Taurine	48.3% (± 7.5)	59.9% (± 10.0)	76.9% (± 5.9)	89.0% (± 4.5)

Product masses for purposes of the calculation were derived from linear fit lines of measured product masses at four concentrations. Each product mass is presented as a percentage of the difference between its predicted maximum and minimum product masses. Maximum standard deviations using actual desiccated mass data are presented as modifiers of the percentile.

Table 3.4. Peaks and vibration modes from Fourier Transform Infrared Spectroscopy spectra.

Vibration mode	Hypotaurine	Taurine	Peroxytaurine
S-O deformation	438		
	452	467	532
	490	524	571
	547	533	584
		599	613
			675
			706
C-S stretch	721	743	741
NH deformation	786	848	802
	832	894	808
		962	883
			960
			1030
C-S=O stretch	938	1038	1049
	962	1113	
	974		
S-O stretch	999	1182	1151
SO_2 stretch		1213	1194
	1047	1222	1251
	1073	1250	1284
	1157	1304	
	1250		
CH bend	1335	1344	1336
CH wag	1377	1388	1384
CH bend	1421	1427	1450
CH bend	1460	1458	1483
	1550	1512	
	1615	1526	
		1586	
NH bend	1639	1617	1593
	2127	2476	1664

Assigned peaks are aligned in rows with indicated vibration mode. Other unassigned peaks are listed in order of frequency (cm^{-1}) and have no particular association with other frequencies in the same row.

Table 3.4. (continued)

Vibration mode	Hypotaurine	Taurine	Peroxytaurine
	2402	2570	1722
		1586	
NH bend	1639	1617	1593
	2127	2476	1664
	2402	2570	1722
		1586	
NH bend	1639	1617	1593
	2127	2476	1664
	2402	2570	1722
		1586	
NH bend	1639	1617	1593
	2127	2476	1664
	2402	2570	1722
		1586	
NH bend	1639	1617	1593

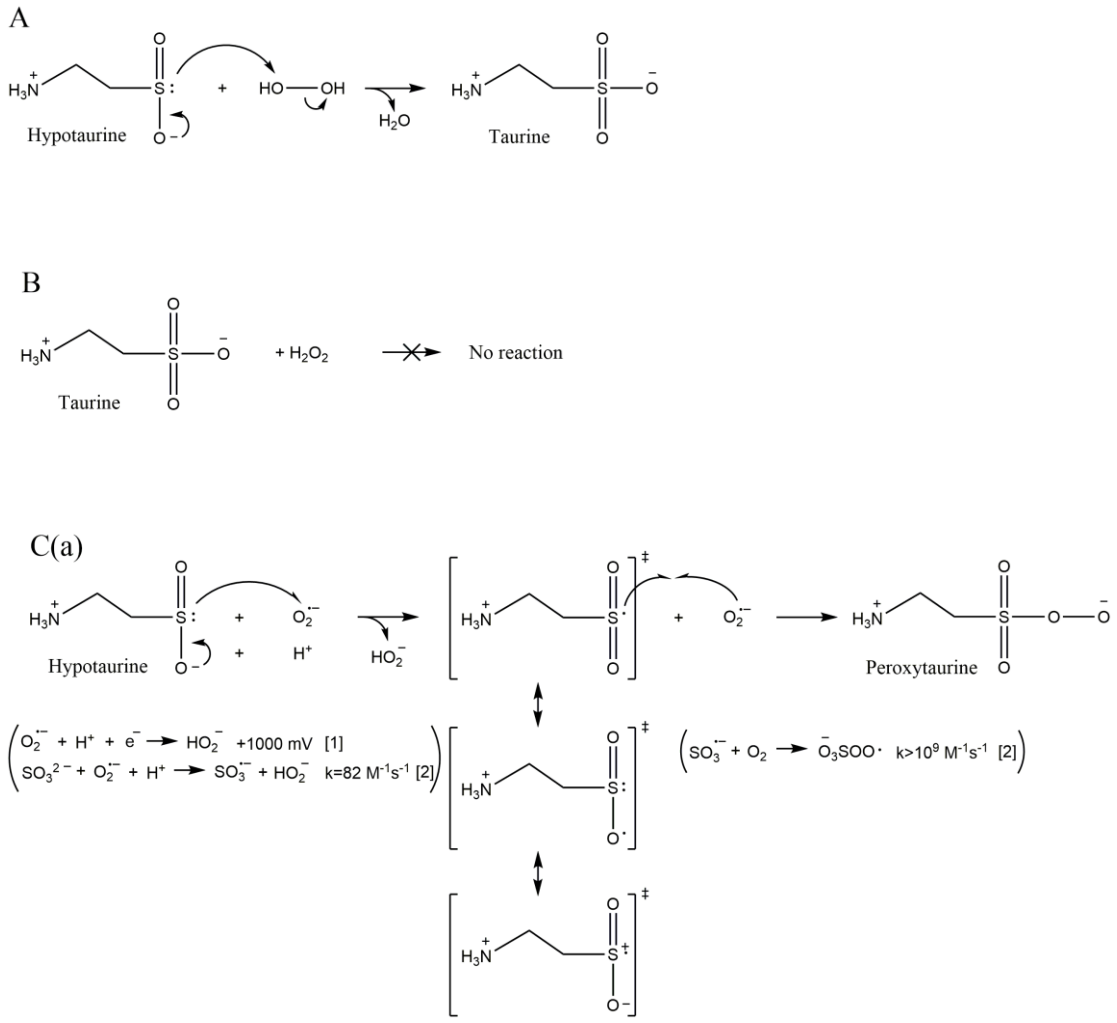

Figure 3.1. Proposal chemical mechanisms involving hypotaurine and taurine. Synthesis reactions are shown involving hypotaurine (A) and taurine (B) with hydrogen peroxide. Two models for the reaction of superoxide with hypotaurine (C(a) and C(b)) and taurine (D(a) and D(b)) are hypothesized. Literature values for standard reduction potential and kinetic data for the presented and analogous reactions are also shown for one electron transfer reactions. Degradation of peroxytaurine (E) is shown. A pH of 7 is assumed in presentation of the protonation state of chemical groups.

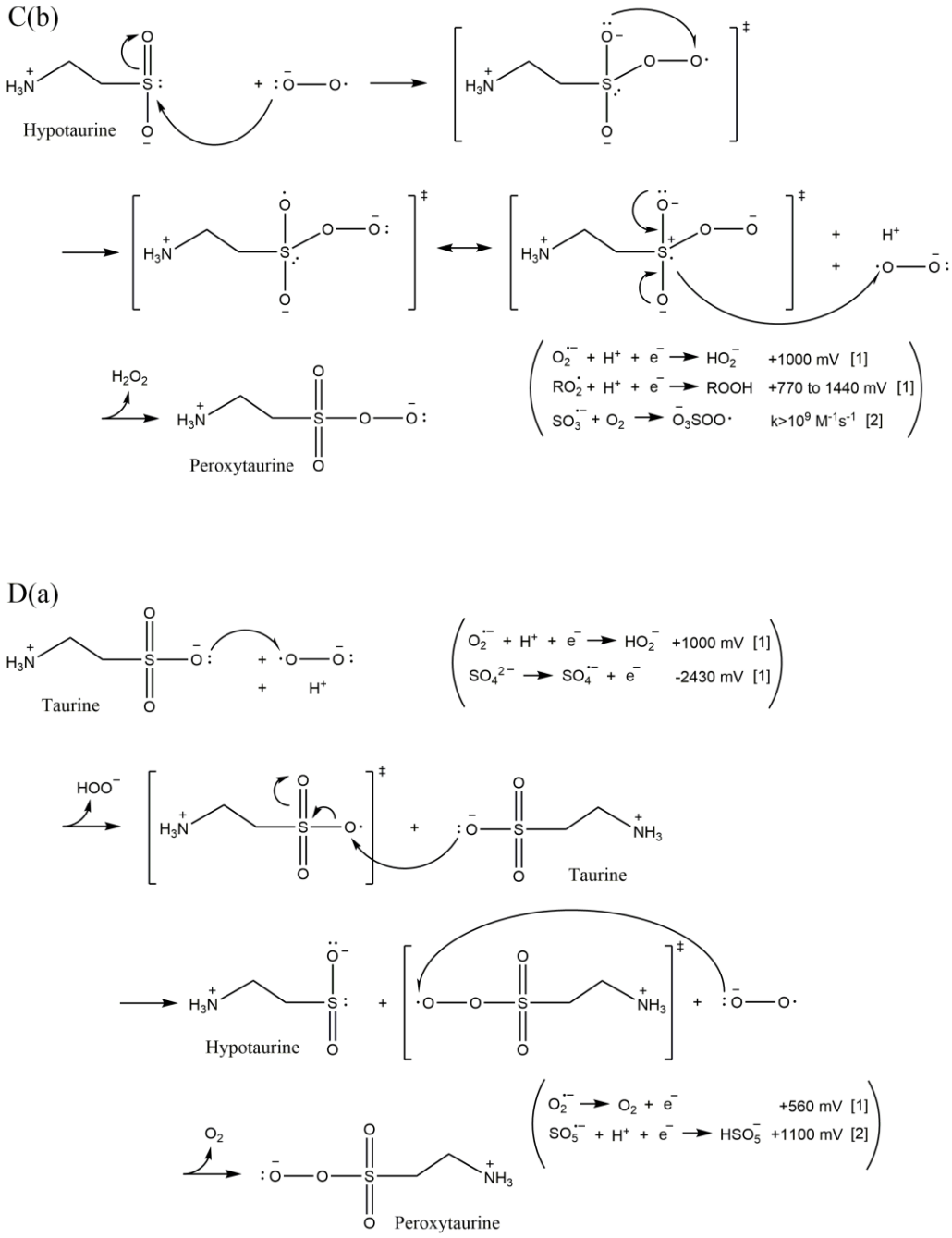

Figure 3.1. Proposal chemical mechanisms involving hypotaurine and taurine (continued).

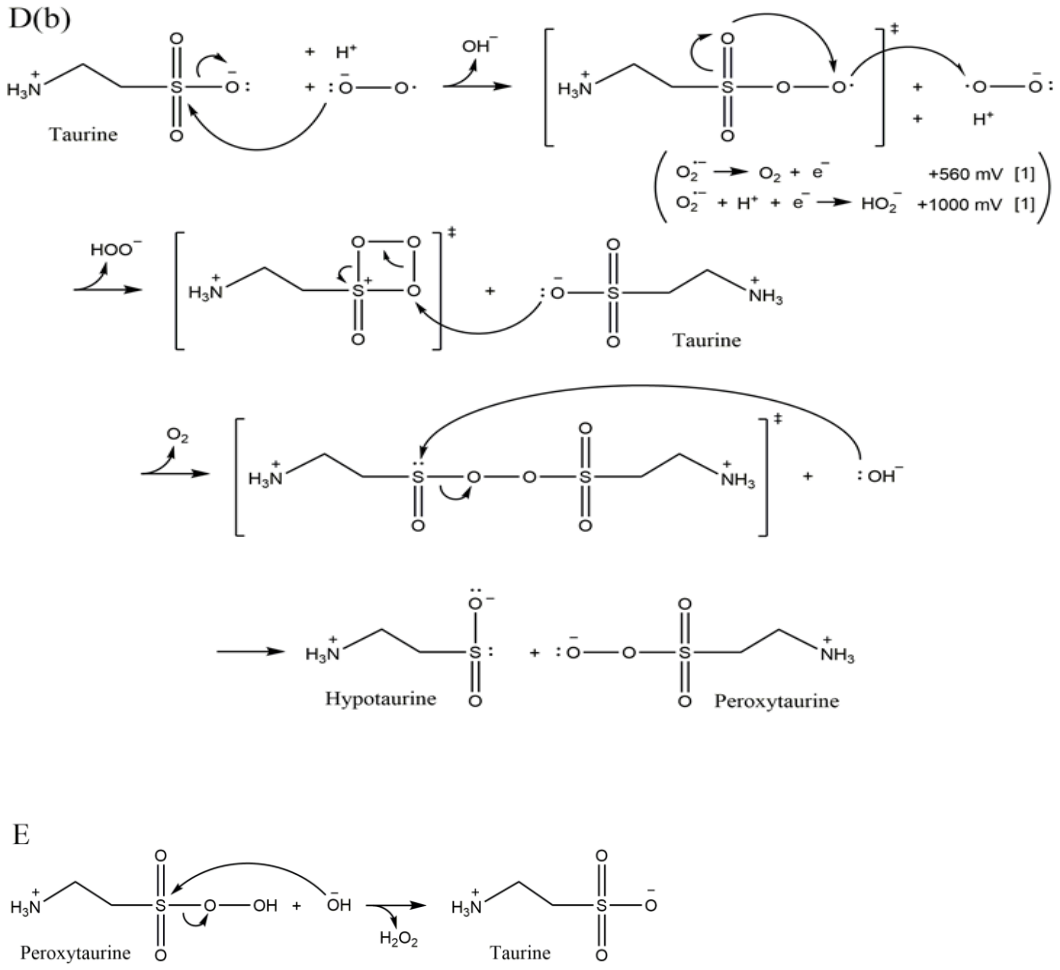

Figure 3.1. Proposal chemical mechanisms involving hypotaurine and taurine (continued).

A.

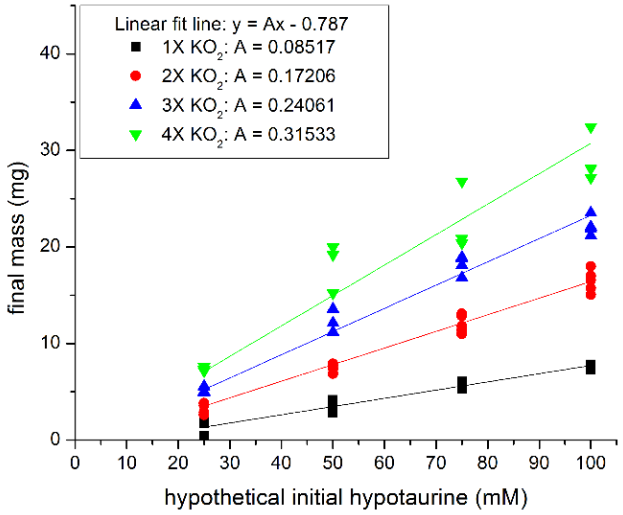

B.

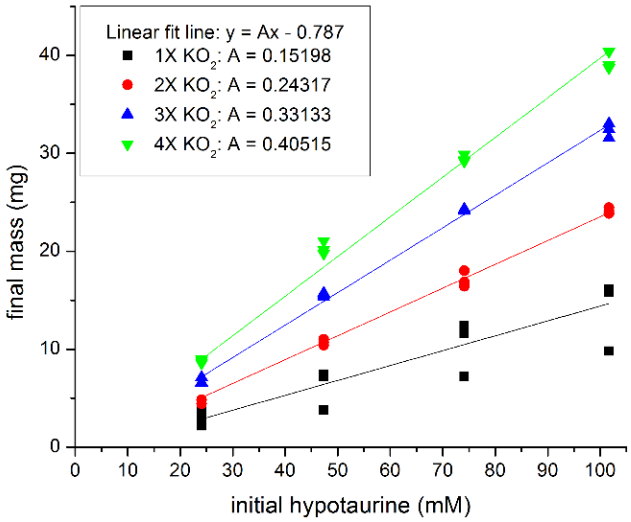

Figure 3.2. Determination of desiccated mass from reaction of hypotaurine to taurine with potassium superoxide. (A) Potassium superoxide was reacted in water alone, and the sample was desiccated by heat. (B) Potassium superoxide was reacted with in solution of hypotaurine before desiccation. (C) Potassium superoxide was reacted in solution of taurine before desiccation. Three or more independent replicates were used for each sample. The negative x-intercept is to correct for systemic error in the balance as measured *via* desiccated water controls.

C.

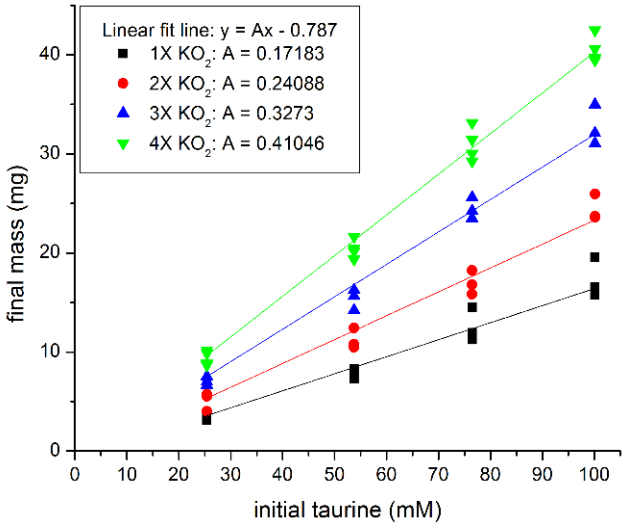

Figure 3.2. (continued)

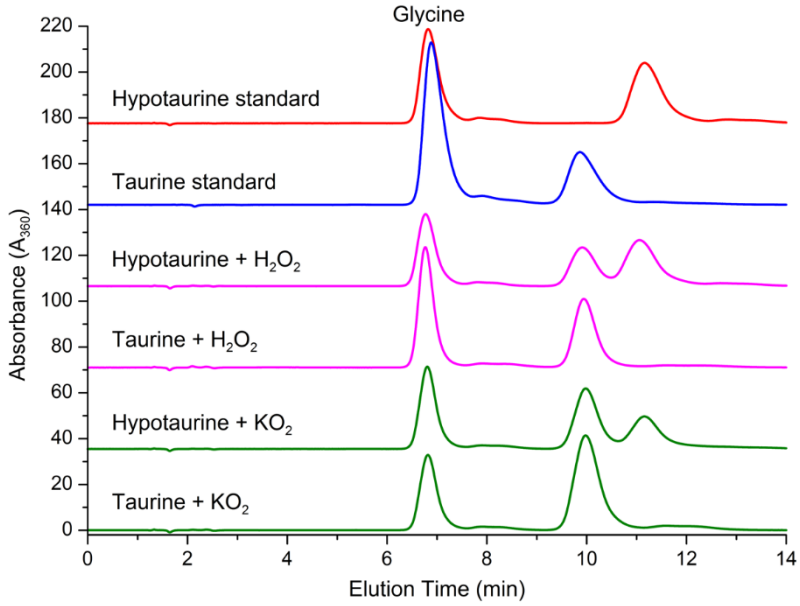

Figure 3.3. High Performance Liquid Chromatography elution times of hypotaurine, taurine, and reaction products. Glycine was added to the solutions as an internal standard immediately before sample injection. Amine-containing molecules were labeled with *ortho*-phthalaldehyde and detected by light absorbance at 360 nm. Three independent replicates were used for each sample in collection of elution time data.

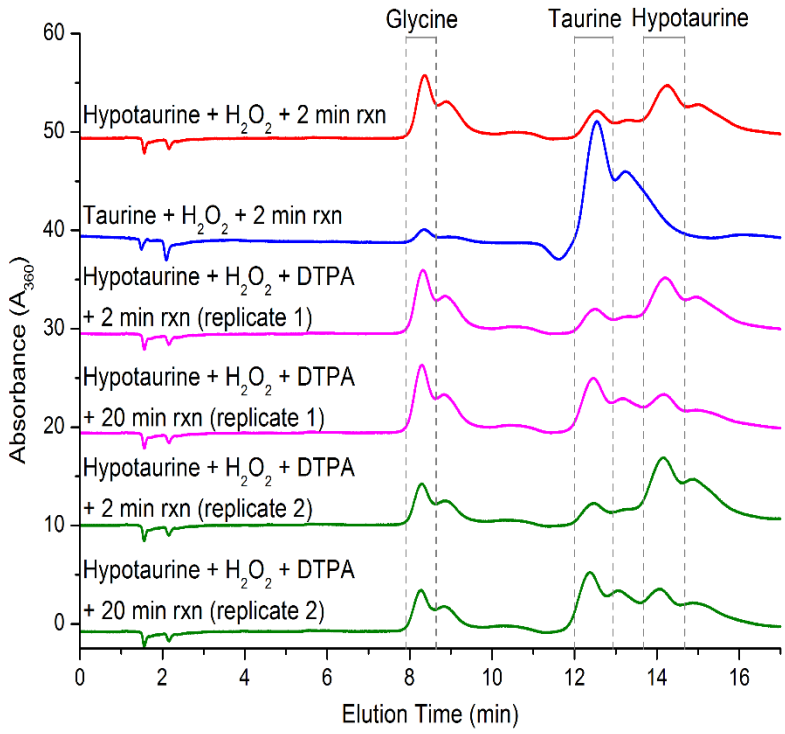

Figure 3.4. High Performance Liquid Chromatography elution times of products from reactions of hypotaurine or taurine with hydrogen peroxide. DTPA was added as a chelating agent. Glycine was added to the solutions as an internal standard immediately before sample injection. Amine-containing molecules were labeled with *orth*-phthalaldehyde and detected by light absorbance at 360 nm. Two independent replicates were used for each sample in collection of elution time data. Elapsed time of reaction before sample injection is given. An unknown disturbance in the HPLC elution system during this experiment resulted in consistent, secondary trailing peaks behind the primary peaks. Primary peaks are enclosed by boxes for clarity.

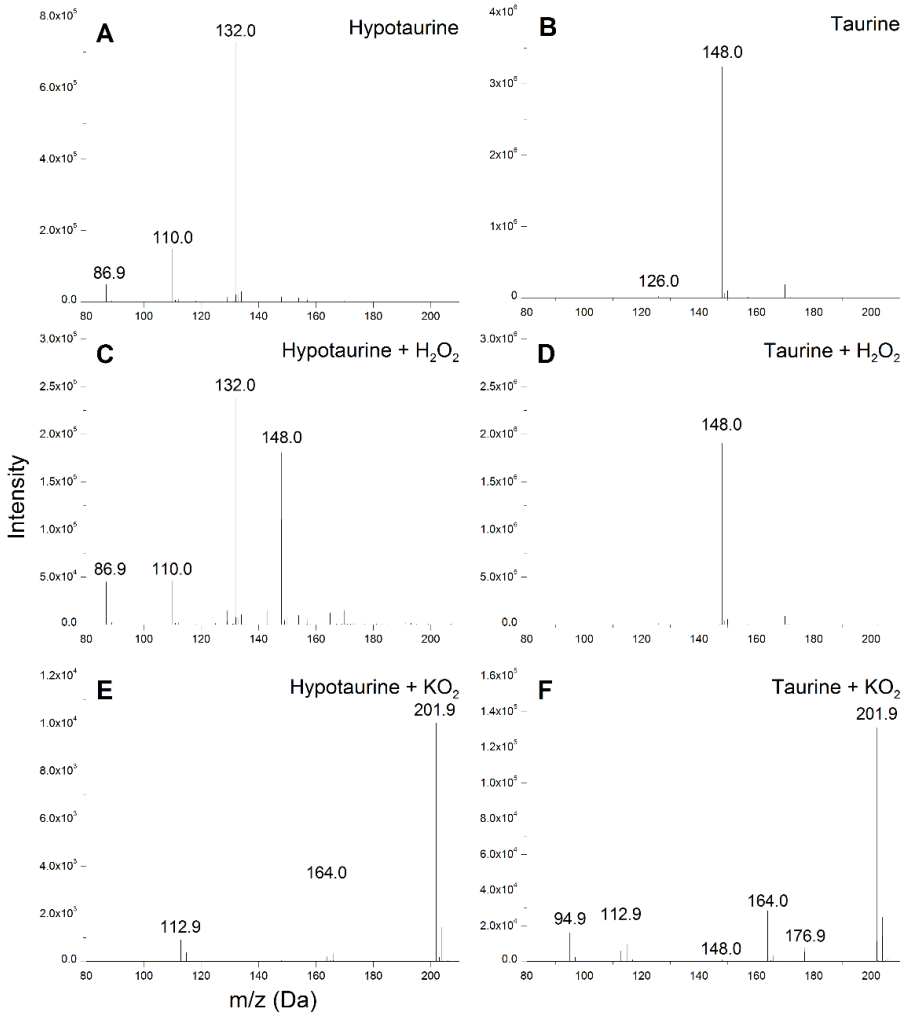

Figure 3.5. Mass Spectrometry spectra for hypotaurine, taurine, and reaction products. An electrospray-ionization setup was used to vaporize liquid samples for detection *via* mass spectrometry. All samples were adjusted to pH 7±1 before injection. Samples in panels A–D were dissolved in phosphate buffer, while samples in panels E–F were dissolved in pure water. Two independent replicates were used for each sample in collection of mass spectrometric data. Intensity counts are arbitrary and not quantitative.

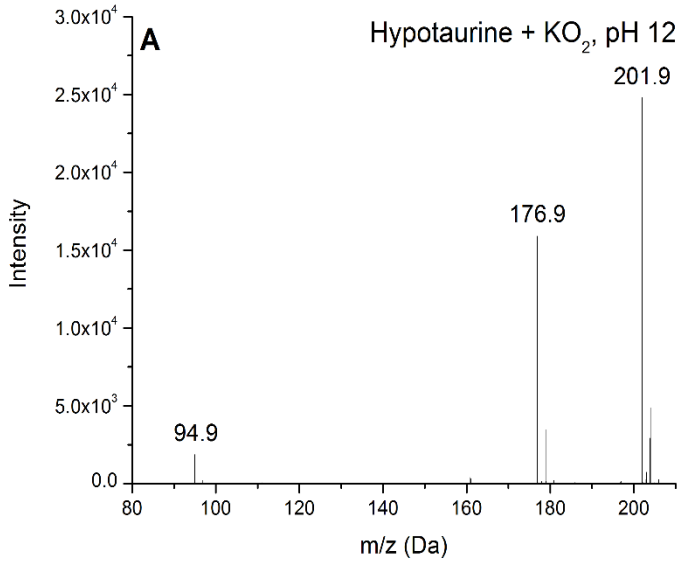

Figure 3.6A. Mass Spectrometry spectra for products from superoxide reactions. An electrospray-ionization setup was used to vaporize liquid samples for detection *via* mass spectrometry. A hypotaurine with superoxide reaction product was not pH-adjusted and was sampled at a pH of 12.

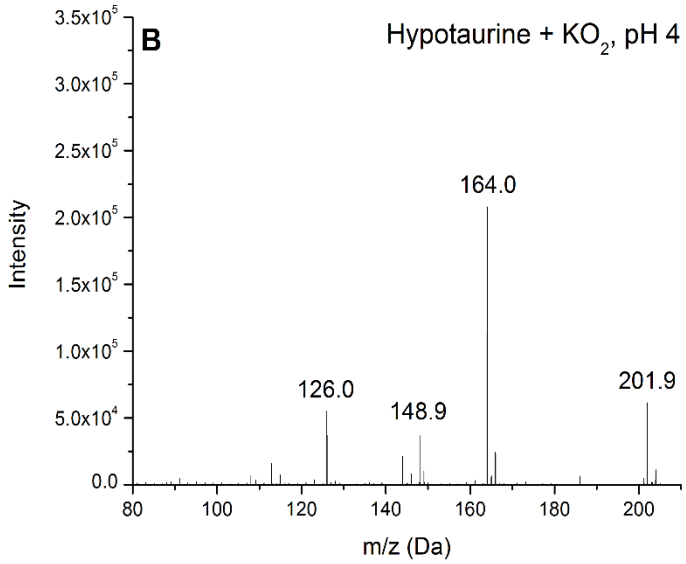

Figure 3.6B. Mass Spectrometry spectra for products from superoxide reactions. An electrospray-ionization setup was used to vaporize liquid samples for detection *via* mass spectrometry. An experimental setup identical to that of part A was performed, except the sample was pH-adjusted to 4.

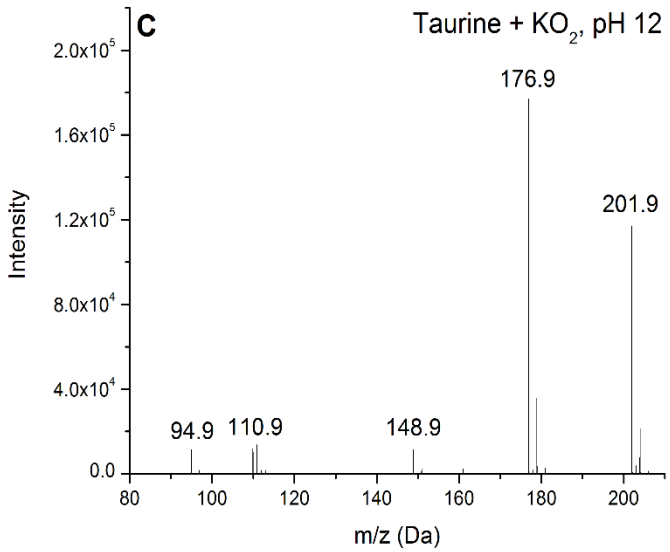

Figure 3.6C. Mass Spectrometry spectra for products from superoxide reactions. An electrospray-ionization setup was used to vaporize liquid samples for detection *via* mass spectrometry. A reaction of taurine with superoxide was not pH-adjusted and was sample at a pH of 12.

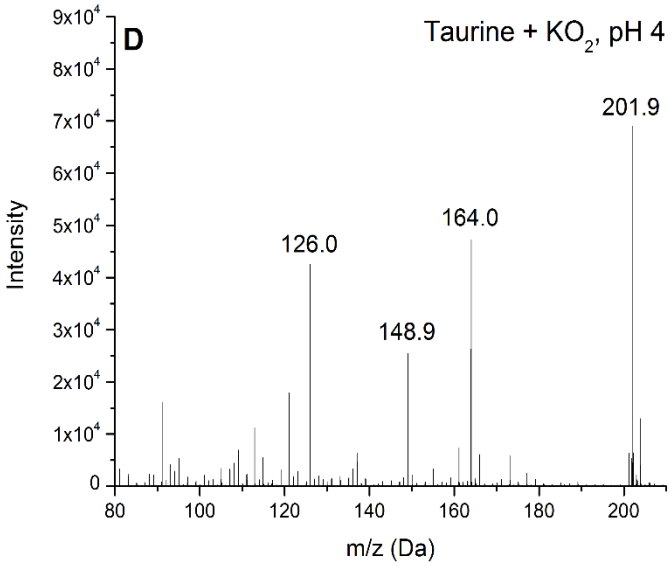

Figure 3.6D. Mass Spectrometry spectra for products from superoxide reactions. An electrospray-ionization setup was used to vaporize liquid samples for detection *via* mass spectrometry. An experimental setup identical to that of part C was performed, except the samples was pH-adjusted to 4.

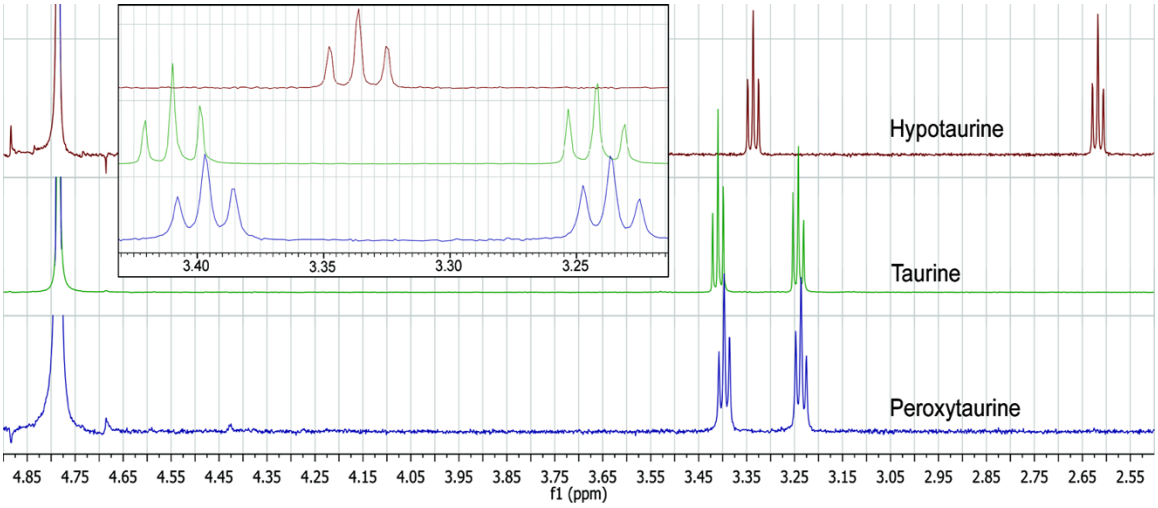

Figure 3.7. ^{1}H-Nuclear Magnetic Resonance Spectrometry spectra of hypotaurine, taurine, and peroxytaurine. Samples were dissolved in D_2O. The peak at 4.785 ppm corresponds to water. The inset amplifies the 3.450–3.200 ppm region.

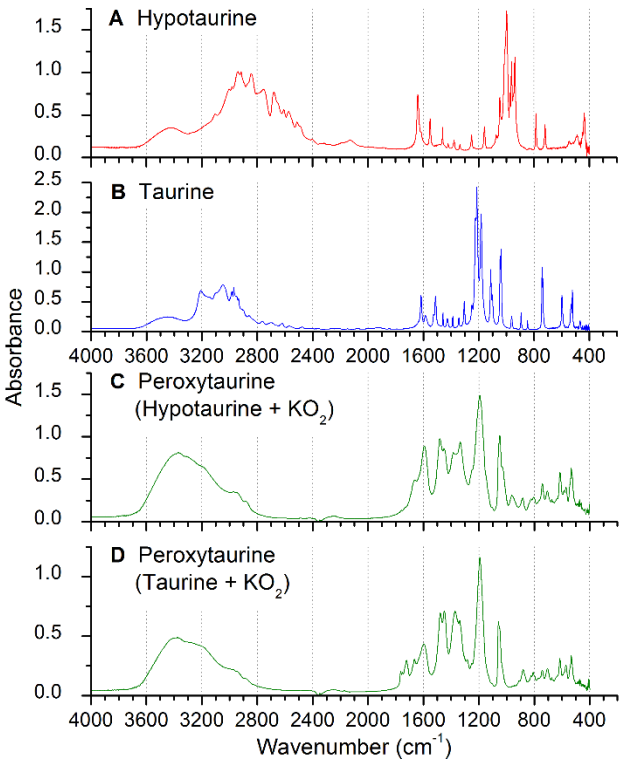

Figure 3.8. Fourier Transform Infrared Spectroscopy spectra for hypotaurine, taurine, and peroxytaurine. Peroxytaurine was produced from the reaction of superoxide with hypotaurine or taurine. Relative absorbance values between samples are dependent on concentration and are thus arbitrary. Three independent replicates were used for each sample in collection of spectra. Representative spectra are presented.

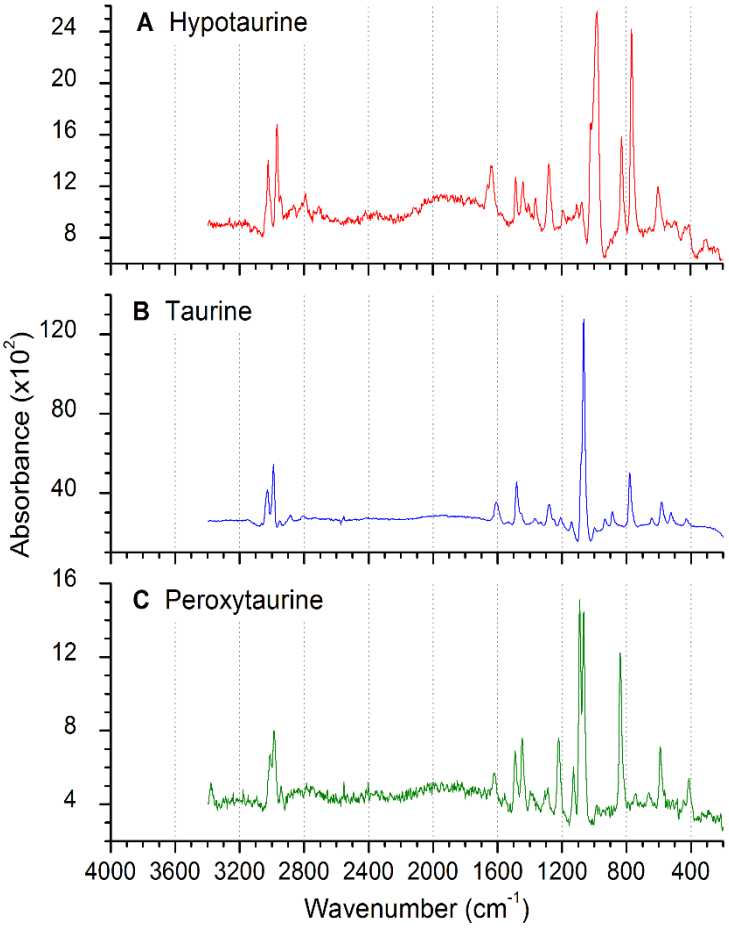

Figure 3.9. Raman Spectroscopy spectra for hypotaurine, taurine, and peroxytaurine. Relative absorbance values between samples are dependent on concentration and thus are arbitrary. Three independent replicates were used for each sample in collection of spectra. Representative spectra are presented.

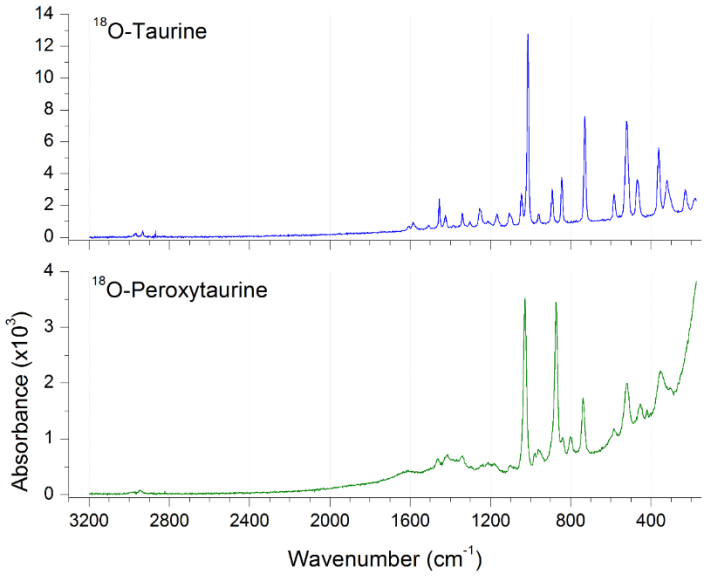

Figure 3.10A. Raman Spectroscopy spectra for ^{18}O isotope-labeled taurine and peroxytaurine. Full spectra of labeled taurine and peroxytaurine. Relative absorbance values between samples are dependent on concentration and have been scaled for purposes of comparison, and thus are arbitrary. Two independent replicates were used for each sample in collection of spectra. Representative spectra are presented.

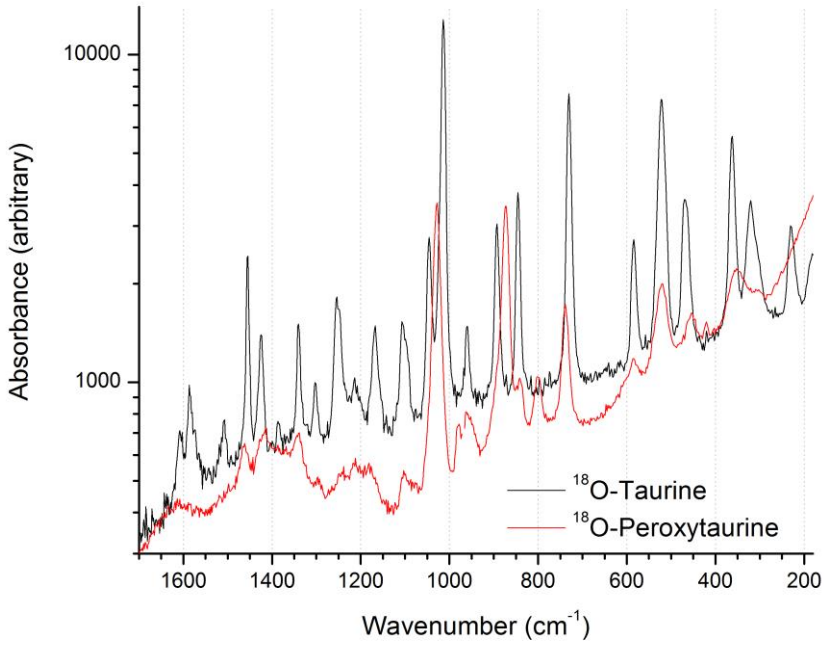

Figure 3.10B. Raman Spectroscopy spectra for ^{18}O isotope-labeled taurine and peroxytaurine. Overlay comparison of taurine and peroxytaurine in region of interest. Relative absorbance values between samples are dependent on concentration and have been scaled for purposes of comparison, and thus are arbitrary. Two independent replicates were used for each sample in collection of spectra. Representative spectra are presented.

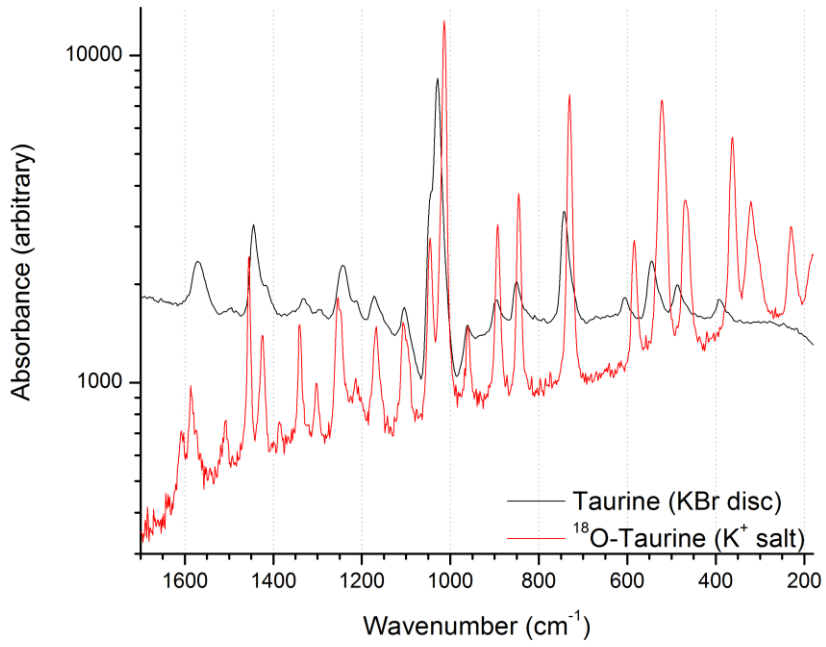

Figure 3.10C. Raman Spectroscopy spectra for ^{18}O isotope-labeled taurine and peroxytaurine. Overlay comparison of labeled and unlabeled taurine. The x-values for unlabeled taurine have been shifted lower by 37 cm^{-1} for purposes of alignment. Relative absorbance values between samples are dependent on concentration and have been scaled for purposes of comparison, and thus are arbitrary. Two independent replicates were used for each sample in collection of spectra. Representative spectra are presented.

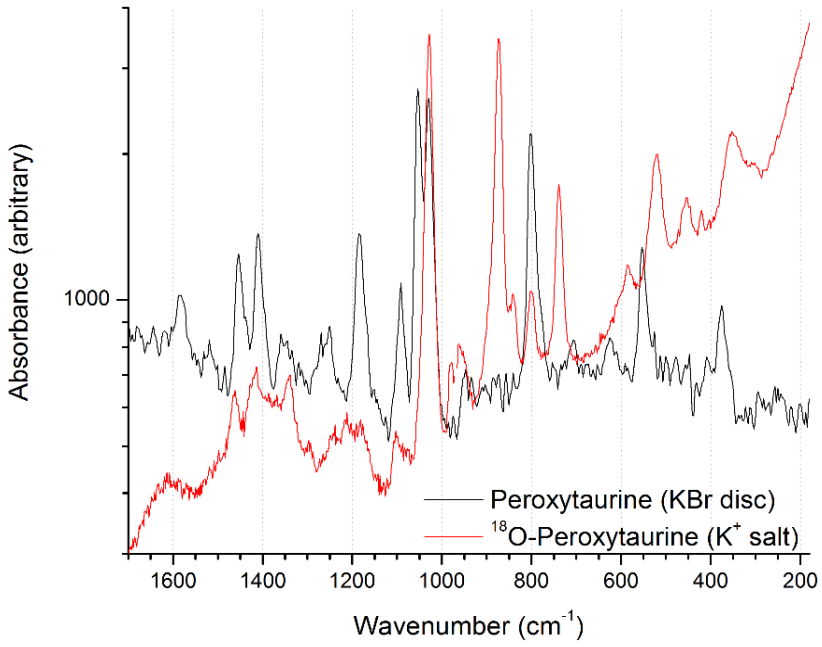

Figure 3.10D. Raman Spectroscopy spectra for ^{18}O isotope-labeled taurine and peroxytaurine. Overlay comparison of labeled and unlabeled peroxytaurine. The x-values for unlabeled peroxytaurine have been shifted lower by 37 cm^{-1} for purposes of alignment. Relative absorbance values between samples are dependent on concentration and have been scaled for purposes of comparison, and thus are arbitrary. Two independent replicates were used for each sample in collection of spectra. Representative spectra are presented.

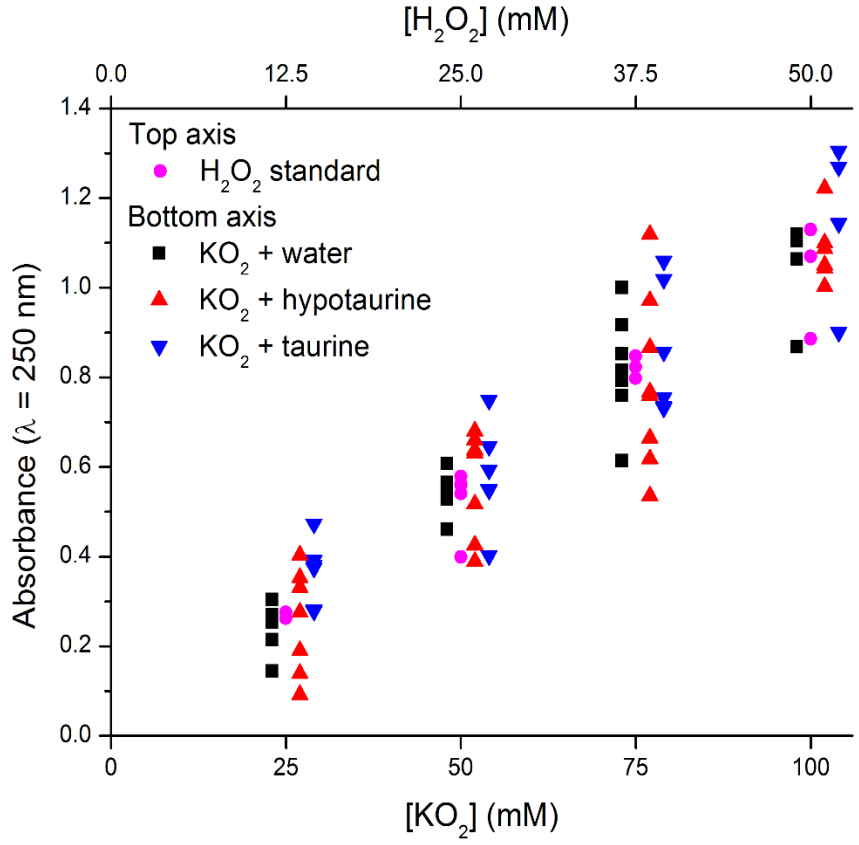

Figure 3.11. Production of hydrogen peroxide by reaction of superoxide in water, 25 mM hypotaurine, or 25 mM taurine solutions. Hydrogen peroxide was measured spectroscopically at 250 nm. Dilutions of a standard solution of hydrogen peroxide provided reference absorbance values at four concentrations. The KO_2 + water, KO_2 + hypotaurine, and KO_2 + taurine values have been offset from the bottom x-axis values of 25, 50, 75 and 100 for the sake of clarity. There is no statistical difference between the mean values of samples at each of the four concentrations.

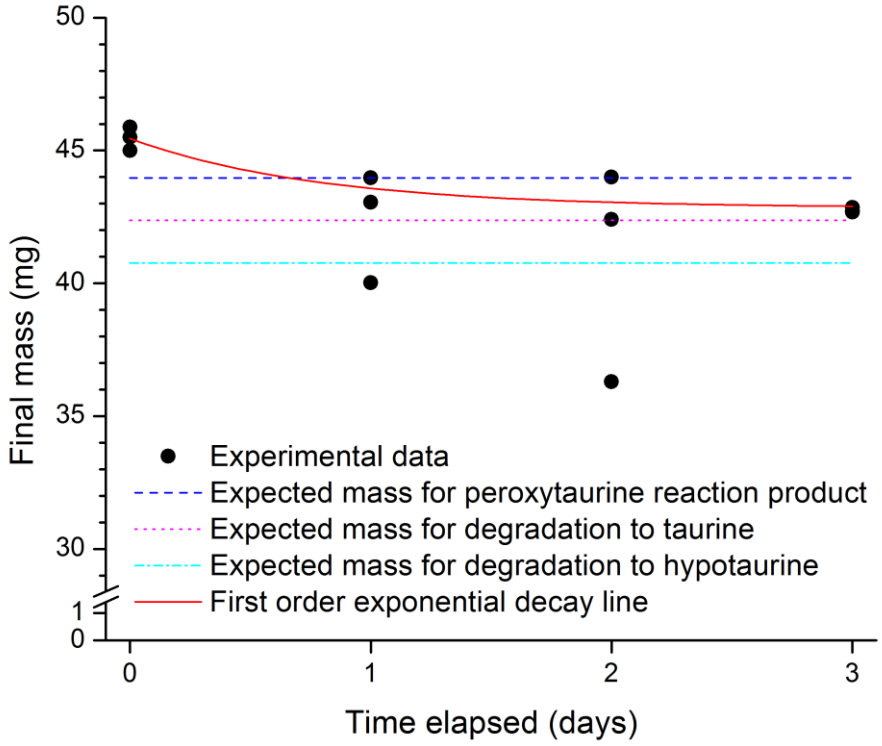

Figure 3.12. Degradation of peroxytaurine in water. Reactions of taurine and 4 molar equivalents potassium superoxide were performed. Samples were pH-adjusted to 7 and treated with catalase, then stored at 24ºC. Samples were desiccated by heat at the indicated time points for determination of mass.

Chapter 4

Investigation of peroxytaurine

I. Introduction

A. Rose Bengal

Various *in vivo* data that taurine has a variety of protective functions and deficiency leads to pathological changes [3]. Taurine has been known as an antioxidant by reacting with hypochlorous acid (HOCl) that is generated at sites of inflammation. Aruoma *et al*. [45] suggested that the precursor of taurine, hypotaurine, might act as an antioxidant *in vivo* by scavenging hydroxyl radicals ($^{\bullet}OH$), and does not react with singlet oxygen ($^1O_2$), but reacts with hydrogen peroxide (H_2O_2). In contrast, Pecci *et al*. [84] suggested that hypotaurine oxidized to taurine by singlet oxygen generated by methylene blue photosensitizer. Grove and Karpowicz [85] observed that hypotaurine reacts with hydrogen peroxide and superoxide and products an intermediate molecule – peroxytaurine.

Reactive oxygen species (ROS) are chemically reactive oxygen-derived molecules, such as hydroxyl radical ($^{\bullet}OH$), superoxide ($^{\bullet}O_2^-$), peroxides (O_2^{2-}) and singlet oxygen ($^1O_2$). Some ROS are free radicals that have an unpaired electron in the outer orbital that can cause cell-damaging reactions, resulting in mutation and injury. ROS plays an essential role in apoptosis induction under physiological and pathological conditions and has destructive actions on DNA and proteins [86].

In vivo, reactive oxygen species (ROS) are formed as a natural byproduct of the normal metabolism of oxygen [87]. During environment stress or exposure to UV light, ROS levels increase and result in cell damage that causes oxidative stress. Among the

free radicals, singlet oxygen has a higher energy state than the triplet ground state molecular oxygen. Singlet oxygen is a toxic gas that causes DNA damage [88].

Singlet oxygen can be produced from porphyrins and Rose Bengal (RB), which are visible light-active photosensitizers [89]. Rose Bengal converts triplet oxygen ($^3O_2$) to singlet oxygen in the presence of light. Once dioxygen is in the singlet excited state, $^1O_2$ becomes more reactive with organic chemical groups. Due to its high electrophilicity, singlet oxygen is capable of oxidizing sulfides and amines.

Singlet oxygen is the active species used in photodynamic therapy, and it is used for sterilizing blood products and in cancer treatment [88]. Photosensitized generation of $^1O_2$ is used for treating wastewater and activating herbicides and insecticides under sunlight [89].

This study was to investigate the antioxidant property of hypotaurine to scavenging singlet oxygen. The hypothesis was that hypotaurine reacts *in vitro* with $^1O_2$ and is oxidized to peroxytaurine.

$$^3O_2 \xrightarrow[\text{photosensitizer}]{\text{light}} {}^1O_2$$

$$\text{Hypotaurine} + {}^1O_2 \xrightarrow{K_c} \text{Peroxytaurine (?)}$$

B. Peroxide Reactions

A novel molecule, peroxytaurine, was discovered from the reaction of hypotaurine with superoxide [85]. The authors used FTIR, NMR, and Raman spectroscopy to confirm that the chemical proprieties of the new molecule are the result of a peroxide group. The distinguishing chemical characteristic of peroxytaurine from

taurine and its analogous molecules is the peroxide group. However, a commercial colorimetric peroxide detection test strips (XPloSens PS, Sigma-Aldrich) designed to detect organic peroxides and other peroxides did not detect peroxytaurine. The strips only detected hydrogen peroxide produced from the formation reaction and the degradation reaction of peroxytaurine. There was no chemical detection observed for the peroxide group in peroxytaurine. The goal of this study was to detect the peroxide group directly in peroxytaurine using chemical reactions.

The chemicals used for this project were acridine, pyridine, and $Fe(II)Cl_2$. The O-O chemical bond of the peroxide is unstable and can be split into reactive radicals via homolytic cleavage. The peroxide may potentially donate an oxygen to acridine and pyridine to form acridine N-oxide and pyridine N-oxide, respectively.

Fenton chemistry is the reaction of hydrogen peroxide with ferrous iron [90]. The peroxide reacts with Fe(II) to form Fe(III) and $OH^{\bullet}$ and OH^{-}. It was hypothesized that Fe(II) would react with peroxytaurine to form Fe(III).

II. Materials and Methods

A. Rose Bengal

All chemical materials were purchased from Sigma–Aldrich (St. Louis, MO, USA). 18.2 MΩ water from Barnstead Nanopure Ultrapure Water Purification System (Thermo Fisher Scientific, Marietta, OH, USA) was used for the preparation of aqueous solutions. A Gemini 3 μm C18 110Å 100 x 4. 6 mm ID column for High Performance Liquid Chromatography was purchased from Phenomenex (Torrance, CA, USA).

Samples and reagents are prepared fresh for every analysis. Reaction mixtures contained 1000 μl of 120 mM hypotaurine, 50 μl of 1 M sodium phosphate buffer pH

7.0, and 200 µl of 300 mM rose Bengal. Reaction mixtures were placed in a quartz cuvette and exposed to ultraviolet light (λ=180 nm) inside a Cary Eclipse Fluorescence Spectrophotometer. The absorbance was set at 540 nm with split width 5 nm. After every 5 min, 300 µl of the mixture solution was combined with 1 µl of 1 M glycine and analyzed by High Performance Liquid Chromatography (HPLC) for hypotaurine and taurine concentrations.

Control solutions were prepared with the same chemical components as the reaction mixture. The solutions were placed in a quartz cuvette and then positioned inside the Cary Eclipse Fluorescence Spectrophotometer without the ultraviolet rays. After mock exposure to ultraviolet light, the solutions were analyzed by HPLC.

Hypotaurine and taurine concentrations were analyzed by reverse-phase HPLC using an Agilent Technologies High Performance 1100 series instrument (Alpharetta, GA, USA), which was equipped with ChemStation software. *ortho*-phthalaldehyde (OPA) with 2-mercaptoethanol was used as a colorimetric tagging agent. Samples were separated by a Gemini 3 µm C18 110 Å 100 x 4.6 mm column. The separation is carried out by a gradient elution at a flow rate of 1.2 ml/min. The elution mixture consisted of 70% of a solution of 0.1 M Na_2HPO_4 and 0.1 mM Na_2-EDTA (pH 6.38) and 30% of methanol. Detection was performed by absorbance at 360 nm. 1 µl of 1 M glycine as an internal standard was added to the mixture solution. Each of the reactions and controls was run in triplicate.

The mixture solution was analyzed by Electrospray Ionization Mass Spectrometry (ESI-MS). ESI-MS was performed on an Applied Biosciences QSTAR Elite hybrid quadrupole/Time Of Flight mass spectrometer system (Foster City, CA, USA), equipped

with a NanoSpray Ion source with Borosilicate Emitters IonSpray Voltage of 1300 V. The samples were analyzed under positive ESI conditions. Analyst QS 2.0 software, using default system parameters, was used to run the instrument. Full scan mass spectra were recorded over the mass range of m/z 50–500 using time-of-flight mode. Nitrogen was used as the curtain and collision gas. The collision energies were between 10 and 25 eV. All spectra reported were averages of 50–200 scans. Each of the reactions and controls were run in triplicate.

B. Peroxide Reactions

Samples and reagents were prepared fresh for every analysis. A standard curve for H_2O_2 was set at 250 mM, 100 mM, 1 mM, 100 µM, 10 µM, and 1 µM. Peroxytaurine solutions were made from hypotaurine and taurine with 3 molar equivalents of potassium superoxide. Peroxytaurine solutions were adjusted to pH 7 ± 1 with 1 N HCl. Catalase was added to the peroxytaurine solution to eliminate background hydrogen peroxide before reacting with acridine, pyridine, or $Fe(II)Cl_2$.

Acridine standard solution at 200 mM was prepared by dissolving acridine in acetic acid and diluted to 100 mM, 10 mM, 1 mM and 0.1 mM. The reactive solutions were prepared by mixing 50 mM peroxytaurine solution with acridine solutions. Pyridine reactive solutions were prepared with the same dilutions as for acridine. Samples were placed in a quartz cuvette and measured on a UV-Vis spectrophotometer (Varian Cary 50 Bio, Agilent Technologies, Santa Clara, CA, USA). Full scan fluorescence spectra were recorded in the wavelength range of 280-500 nm.

Standard $Fe(II)Cl_2$ solution was prepared at 200 µM in water and 100 µM taurine. $Fe(II)Cl_2$ reaction solutions were prepared with peroxytaurine. After 30 seconds, the

reaction solutions were placed in plastic cuvettes and measured on a Varian Cary 50 UV-Vis spectrometry. Full scan fluorescence spectra were recorded in the wavelength range of 250-800 nm.

III. Results and Discussion

A. Rose Bengal

The reaction of hypotaurine with singlet oxygen was investigated. Rose Bengal exhibits intense absorption bands in the green area of the visible spectrum (480-550 nm). Reaction mixtures of Rose Bengal and hypotaurine in buffer solution were placed in a quartz cuvette and then exposed to ultraviolet rays inside a Cary Eclipse Fluorescence Spectrophotometer. The absorbance was set at 540 nm. After 15 or 30 minutes, 300 µl of the mixture solution was combined with 1 µl of 1 M glycine and analyzed by HPLC assay for hypotaurine and taurine concentrations.

The reaction solutions of hypotaurine and Rose Bengal were isolated by HPLC. Glycine eluted at 11 min and served as an internal control (Figure 4.1). Hypotaurine eluted at 20 min and taurine at 16 min. There appeared to be taurine peaks detected at 16 min after the mixture solution exposure to 30 minutes of UV light.

To confirm if there was a taurine product from the reaction of Rose Bengal and hypotaurine, an electrospray ionization-mass spectrometry (ESI-MS) experiment was performed. A reaction solution (pH ~7) revealed a hypotaurine peak at 132 *m/z* (Figure 4.2A) and a taurine peak at 148 *m/z* (Figure 4.2B). The reaction solution (pH~7) of hypotaurine and Rose Bengal after exposure to ultraviolet light for 30 min revealed peaks at 132 *m/z* and 148 *m/z* (Figure 4.C). The small peak of 148 *m/z* (Figure 4.2C) was also observed in the hypotaurine control (Figure 4.2A). The 148 *m/z* peak was small, probably

occurred due to background oxidation, and was not enough to demonstrate the presence of the taurine reaction product.

It was unclear regarding why the taurine peak appeared in the HPLC from the reaction mixture of Rose Bengal and hypotaurine (Figure 4.1). It may be due to the degradation of the OPA solution or carry over from the previous sample. ESI-MS provided more convincing evidence that little or no taurine was produced from the reaction mixture. The small peak of 148 *m/z* in Figure 4.2C was not enough to conclude that hypotaurine reacts with singlet oxygen from Rose Bengal to produce taurine. This study agrees with a previous study [45] that showed hypotaurine does not react with singlet oxygen but disagrees with another study [84] that hypotaurine reacts with singlet oxygen.

B. Peroxide Reactions

The hypothesized chemical reactions of hypotaurine with acridine or pyridine was to form acridine N-oxide (Figure 4.3A) and pyridine N-oxide, respectively. UV-vis absorption spectra of acridine and pyridine have absorbance maxima at 350 nm and 256 nm, respectively [91]. Acridine N-oxide has absorbance maxima at 400 nm, 425 and 480 nm [92]. Pyridine N-oxide has an absorbance maximum at 338 nm. Data showed there were no new peaks detected at 400 nm, 425 nm, and 480 nm when reacting peroxytaurine with acridine, which indicated that no N-oxide was formed (Figure 4.4). The lower intensity of the 350 nm peak of 100 mM acridine with 50 mM peroxytaurine compared to 100 mM acridine alone suggested that peroxytaurine reacted with acridine but not in the way that was expected (Figure 4.3A). The presence of no new peaks indicated there was no N-oxide formed. The reaction of acridine and peroxytaurine can be explained as by

nucleophilic attack on acridine at position 9 to break the aromatic ring and form an aldehyde [93] (Figure 4.3B).

In the case of pyridine, there was no change in signal from the spectra peaks (data not shown), which indicated no reaction occurred. The conclusion from the spectra is that peroxytaurine has weaker oxidation potential than other peroxy acids and cannot form N-oxide with acridine or pyridine. However, it still appears to react with acridine and form a different product than expected.

Figure 4.5 shows the UV-Vis absorption spectra of the reaction of different concentrations of iron and peroxytaurine. Fe^{2+} absorbs light from 240 to 280 nm, and Fe^{3+} from 300 to 350 nm [94]. Fe^{2+} reacted with peroxytaurine to form the product Fe^{3+}, and the absorbance was measured at 350 nm. Hydrogen peroxide (H_2O_2) reacts with Fe^{2+} to form Fe^{3+}. H_2O_2 has absorbance from 185 nm to 220 nm (data not shown). Therefore, it was necessary to add catalase to the peroxytaurine solution to eliminate any background H_2O_2. After catalase was added, the solution formed bubbles, which indicated the hydrogen peroxide was breaking down to water and releasing oxygen. The data shows that the same concentration of Fe^{2+} (200 μM) had a higher intensity in the range of 300 to 400 nm when mixed with peroxytaurine compared to H_2O. The data showed that Fe^{2+} converted to Fe^{3+}, which confirmed that the peroxide in peroxytaurine reacted with Fe^{2+}.

$$Fe^{2+} + O_2^{2-} + 2H^+ \Longrightarrow Fe^{3+} + OH^{\bullet} + OH^-$$

The conclusion from the results of the acridine, pyridine, and Fe(II) experiments provided direct chemical evidence of the presence of a peroxide in peroxytaurine.

IV. Figures

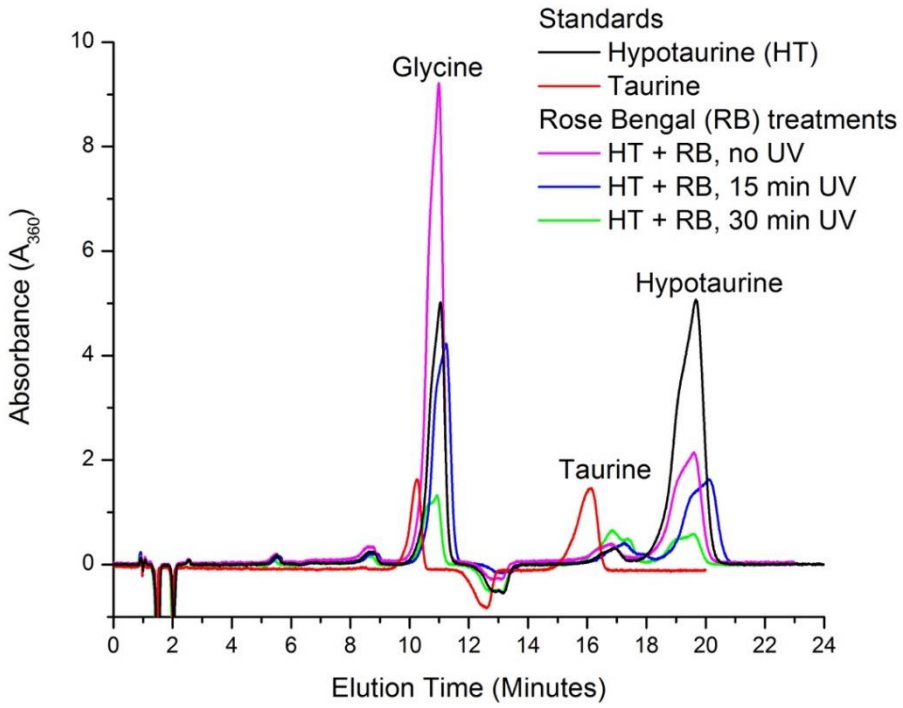

Figure 4.1. High Performance Liquid Chromatography shows elution of hypotaurine, taurine and the reaction products of hypotaurine and Rose Bengal before and after exposure to UV. Glycine was added to the solution as an internal standard immediately before sample injection. Amine-containing molecules were labeled with *ortho*-phthalaldehyde and detected by light absorbance at 360 nm.

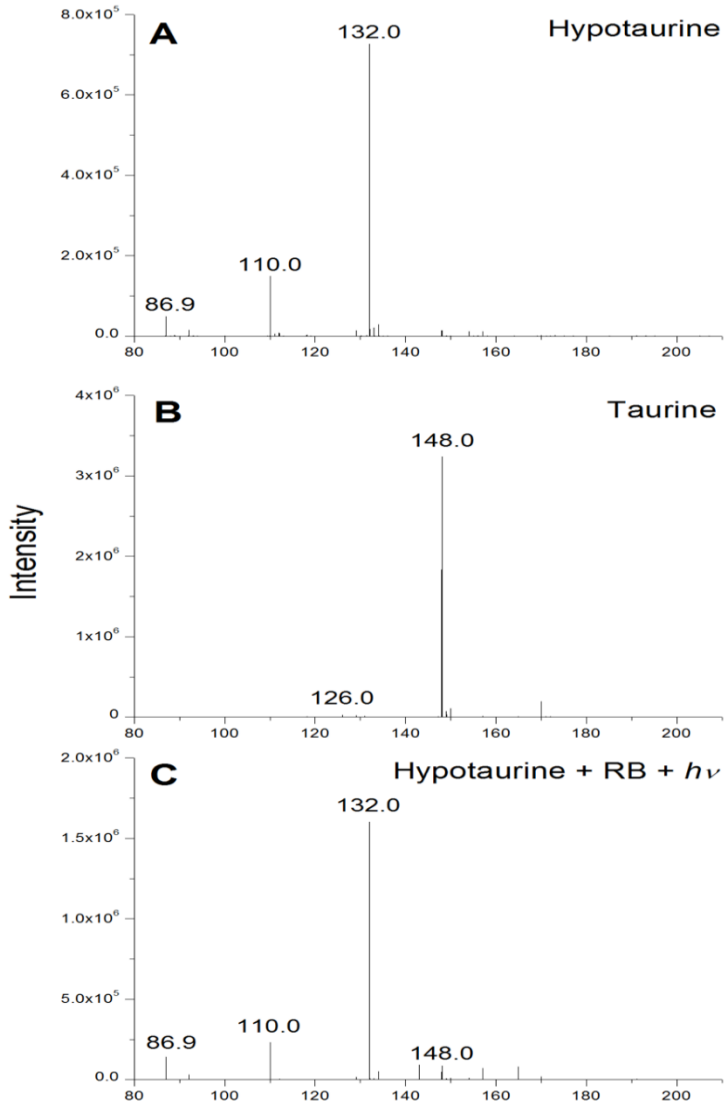

Figure 4.2. ESI-MS spectra for (A) hypotaurine, (B) taurine and (C) reaction solution of hypotaurine with Rose Bengal after exposure to UV for 30 min. An electrospray-ionization setup was used to vaporize liquid samples for detection of positive ions via mass spectrometry. All samples were adjusted to pH 7 ± 1 before injection. Intensity counts are arbitrary and not quantitative.

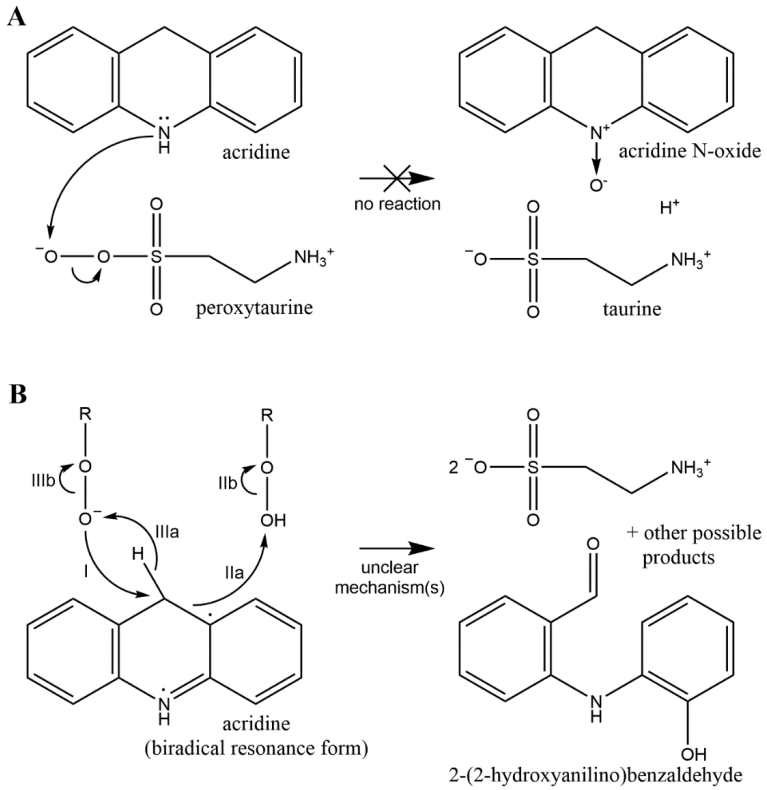

Figure 4.3. Proposed chemical reactions involving acridine with peroxytaurine (A) Expected reaction of peroxytaurine with acridine forms N-oxide and taurine (B) Acridine undergoes nucleophilic attack at position 9, which breaks the aromatic ring and forms an aldehyde.

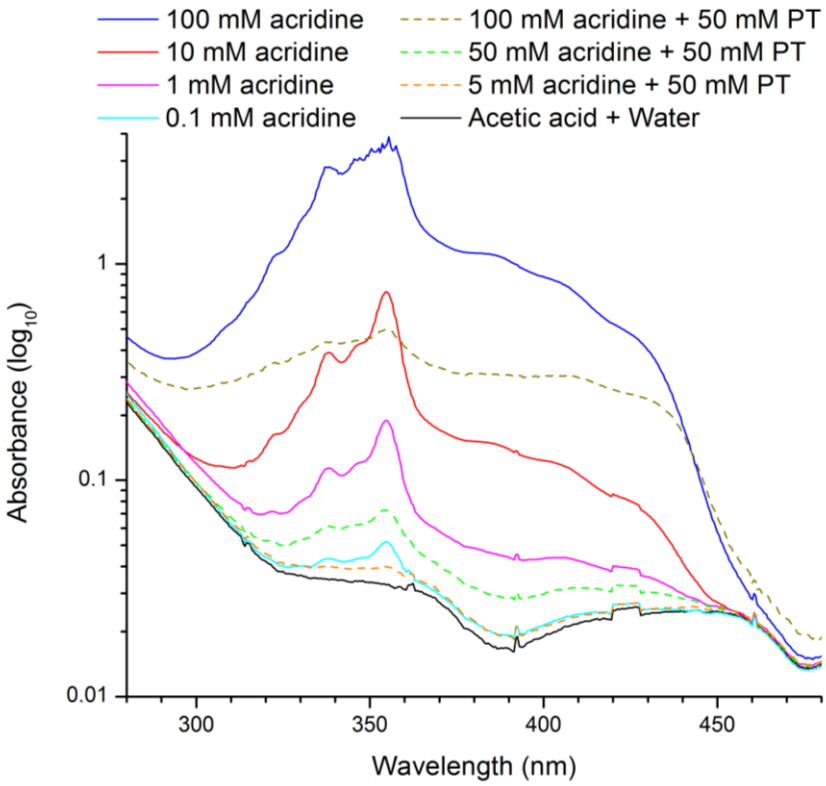

Figure 4.4. UV-Visible absorbance spectra of acridine standard and acridine with peroxytaurine. Acridine solutions were prepared by dissolving acridine in acetic acid. Peroxytaurine solutions were adjusted to pH 7 ± 1. Catalase was added to the solutions to eliminate H_2O_2 before reaction with acridine.

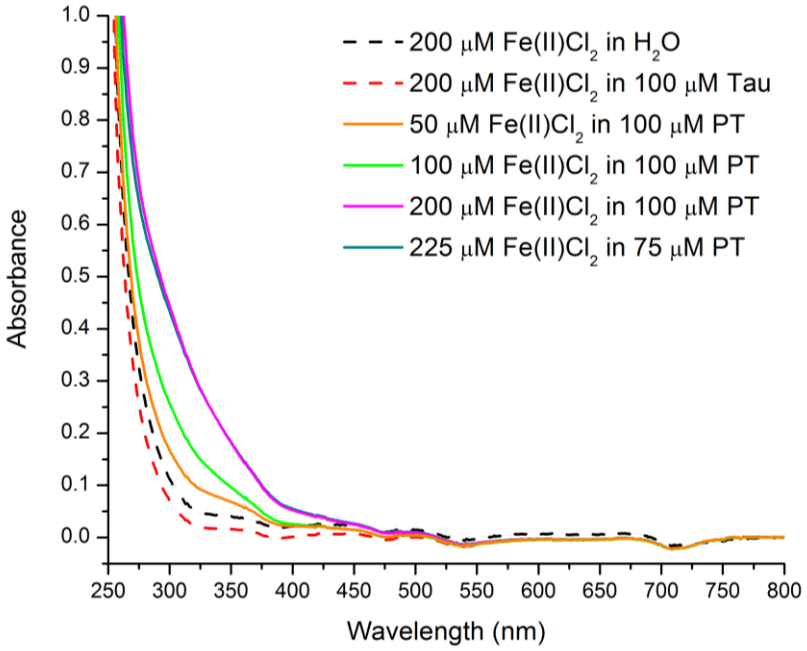

Figure 4.5. UV-visible spectra of $Fe(II)Cl_2$ in the solution of water, taurine, and peroxytaurine. Catalase was added to the solutions to eliminate H_2O_2 before reaction with $Fe(II)Cl_2$.

Chapter 5

General Summary

Taurine, an amino acid-derived molecule, has fascinated scientists for decades. Knowledge of the biological roles and biochemical functions of taurine remain elusive despite decades of studies and investigations [4]. The goal of this projects was to understand the biosynthesis reaction of taurine better.

The initial plan was to identify the gene and protein involved in the conversion of hypotaurine to taurine and perform protein expression and screening for protein activity. Bioinformatic analysis of over 100 genes from three species from GeneNetwork and COXPRESdb database indicated that flavin-containing monooxygenase (FMO) genes were highly correlated with CDO1, CSAD, and ADO. Co-factors NAD^+ and NADPH were added with hypotaurine to cell lysate to observe the presence of an enzyme that could catalyze the reaction of hypotaurine to taurine. The cell lysates were analyzed using High Performance Liquid Chromatography for additional taurine production. Results from HPLC revealed no change in taurine concentration which suggested this line of experimentation was not promising. For that reason, alternative pursuits were used to investigate non-enzymatic reactions.

HPLC is the most common method for measuring taurine concentration. Although gas chromatography had been used to measure taurine in some studies [95], the attempt to use a gas chromatography method in this project failed because taurine is poorly soluble in common solvents other than water and taurine is not volatile.

Reactions of hypotaurine and taurine with hydrogen peroxide, superoxide, and singlet oxygen were observed from HPLC and ElectroSpray Ionization -Mass

Spectrometry. Mass spectrometry revealed a novel molecule that peaks at 164 *m/z,* which corresponds to the mass of a hypotaurine (132 m/z) plus two oxygen atoms (32 m/z). Evidence from Fourier Transform Infrared Spectroscopy, Nuclear Magnetic Resonance Spectroscopy, and Raman Spectrometry suggested chemical properties indicating the novel molecule peroxytaurine which has a peroxy acid. FTIR and Raman spectrometry were performed with an ^{18}O isotope labeled peroxytaurine to confirm the presence of the O-O bond of the peroxy acid. The results suggested that hypotaurine and taurine are oxidized to peroxytaurine. Hypotaurine reacts with hydrogen peroxide and converts to taurine. Hypotaurine did not oxidize in the presence of Rose Bengal, which is a singlet oxygen generator.

To further investigate the presence of the peroxy acid in peroxytaurine, direct chemical reactions of peroxytaurine with pyridine, acridine, and $Fe(II)Cl_2$ were also studied. Although UV-vis spectra showed no presence of acridine N-oxide or pyridine N-oxide as predicted, a different product may have been formed from the reaction of peroxytaurine with acridine. Peroxytaurine reacted with Fe(II) to produce Fe(III).

Since peroxytaurine has a similar chemical structure to taurine and is only an oxygen atom different in mass, therefore, was observed to have approximately the same elution time as taurine on HPLC. This observation explains why no one had previously identified peroxytaurine. No one had ever used ESI-MS, FTIR, and Raman spectrometry to analyze hypotaurine and taurine compounds.

Although no new gene or protein was identified, the discovery of the peroxytaurine molecule demonstrated that there is a spontaneous intermediate reaction in

the conversion of hypotaurine to taurine. Further analysis of peroxytaurine will contribute to the understanding of the metabolism of taurine.

Literature Cited

1. Xu YJ, Arneja AS, Tappia PS, Dhalla NS: **The potential health benefits of taurine in cardiovascular disease**. *Experimental & Clinical Cardiology* 2008, **13**(2):57.
2. Rips H, Shen W: **Taurine: A "very essential" amino acid**. *Molecular Vision* 2012, **18**:5-17.
3. Huxtable RJ: **Physiological actions of taurine**. *Physiological Reviews* 1992, **72**(1):101-163.
4. Jacobsen JG, Smith Jr LH: **Biochemistry and physiology of taurine and taurine derivatives**. *Physiological Reviews* 1968, **48**:424-511.
5. Stipanuk MH, Jurkowska H, Roman HB, Niewiadomski J, Hirschberger LL: **Insights into taurine synthesis and function based on studies with cysteine dioxygenase (CDO1) knockout mice**. *In Taurine 9* 2015:29-39.
6. Stipanuk MH, Coloso RM, Garcia RA, Banks MF: **Cysteine concentration regulates cysteine metabolism to glutathione, sulfate, and taurine in rat hepatocytes**. *The Journal of Nutrition* 2004, **122**(3):420-427.
7. Brand A, Leibfritz D, Hamprect B, Dringen R: **Metabolism of cysteine in astroglial cells: Synthesis of hypotaurine and taurine**. *Journal of Neurochemistry* 1998, **71**(2):827-832.
8. Yancey PH, Ishikawa J, Meyer B, Girguis PR, Lee RW: **Thiotaurine and hypotaurine contents in hydrothermal-vent polychaetes Without thiotrophic endosymbionts: Correlation with sulfide exposure**. *Journal of Experimental Zoology*, 2009, **311**:439-447.

9. Sturman JA, Gaull GE: **Taurine in the brain and liver of the developing human and monkey**. *Journal of Neurochemistry* 1975, **25**(6):831-835.

10. Sturman JA: **Taurine in development**. *Physiol Rev* 1993, **73**:119-147.

11. Lourenco R, Camilo ME: **Taurine: a conditionally essential amino acid in humans? An overview in health and disease**. *Nutr Hosp* 2002, **17**(6):262-270.

12. Locke D, Kieken F, Tao L, Sorgen PL, Harris AL: **Mechanism for modulation of gating of connexin26-containing channels by taurine**. *The Journal of General Physiology* 2011, **138**(3):321-339.

13. Anderson CMH, Howard A, Walters JRF, Ganapathy V, Thwaites DT: **Taurine uptake across the human intestinal brush-border membrane is via two transporters: H+-coupled PAT1 (SLC36A1) and Na+- and Cl−-dependent TauT (SLC6A6).** . *The Journal of Physiology* 2009, **587**(4):731-744.

14. Hayes KC, Sturman JA: **Taurine in metabolism**. *Annual Review of Nutrition* 1981, **1**(1):401-425.

15. Froger N, Moutsimilli L, Cadetti L, Jammoul F, Wang QP, Fan Y, Gaucher D, Rosolean SG, Neveux N, Cynober L *et al*: **Taurine: the comeback of a neutraceutical in the prevention of retinal degenerations**. *Progress in Retinal and Eye Research* 2014, **41**:44-63.

16. Brand A, Leibfritz D, Hamprect B, Dringen R: **Synthesis of the organic osmolytes hypotaurine and taurine in astroglial cells**. *Institute for Organic Chemistry* 1998, **107**:13-14.

17. Marnela KM, Morris HR, Panico M, Timonen M, Lahdesmaki P: **Glutamyl-taurine is the predominant synaptic taurine peptide**. *J Neurochem* 1985, **44**:752-754.

18. L'Amoreaux W: **The role of taurine in the retina**. *Taurine in Health and Disease* 2012:215-254.

19. Giordano C, Sansone A, Masi A, Masci A, Mosca L, Chiaraluce R, Pasquo A, Consalvi V: **Inhibition of Amyloid Peptide Fragment Aß25-35 Fibrillogenesis and Toxicity by N-Terminal ß Amino Acid Containing Esapeptides: Is Taurine Moiety Essential for In Vivo Effects?** . *Chemical Biology & Drug Design* 2012, **79**(1):30-37.

20. Barakat L, Wang D, Bordey A: **Carrier-mediated uptake and release of taurine from Bergmann glia in rat cerebellar slices**. *The Journal of Physiology* 2002, **541**(3):753-767.

21. Cook AM, Denger K: **Dissimilation of the C2 sulfonates**. *Archives of Microbiology* 2002, **179**(1):1-6.

22. Felux AK, Denger K, Weiss M, Cook AM, Schleheck D: **Paracoccus denitrificans PD1222 utilizes hypotaurine via transamination followed by spontaneous desulfination to yield acetaldehyde and, finally, acetate for growth**. *Journal of Bacteriology* 2013, **195**(12):2921-2930.

23. Denger K, Laue H, Cook AM: **Anaerobic taurine oxidation: a novel reaction by a nitrate-reducing Alcaligenes sp**. *Microbiology* 1997, **143**(6):1919-1924.

24. Eichhorn E, van der Ploeg JR, Kertesz MA, Leisinger T: **Characterization of α-ketoglutarate-dependent taurine dioxygenase from Escherichia coli**. *Journal of Biological Chemistry* 1997, **272**(37):23031-23036.

25. Ruff J, Denger K, Cook AM: **Sulphoacetaldehyde acetyltransferase yields acetyl phosphate: purification from Alcaligenes defragrans and gene clusters in taurine degradation**. *Biochemical Journal* 2003, **369**(2):275-285.

26. Laue H, Friedrich M, Ruff J, Cook AM: **Dissimilatory sulfite reductase (desulfoviridin) of the taurine-degrading, non-sulfate-reducing bacterium Bilophila wadsworthia RZATAU contains a fused DsrB-DsrD subunit**. *Journal of Bacteriology* 2001, **183**(5):1727-1733.

27. Heubi JE, Setchell KD, Bove KE: **Inborn errors of bile acid metabolism.** . *In Seminars in Liver Disease* 2007, **27**(03):282-294.

28. Guglielmi FW, Regano N, Mazzuoli S, Fregnan S, Leogrande G, Guglielmi A, Merli M, Pironi L, Penco JM, Francavilla A: **Cholestasis induced by total parenteral nutrition**. *Clinics in Liver Disease* 2008, **12**(1):97-110.

29. Suzuki T, Suzuki T, Wada T, Saigo K, Watanabe K: **Taurine as a constituent of mitochondrial tRNAs: new insights into the functions of taurine and human mitochondrial diseases**. *EMBO Journal* 2002, **21**:6581-6589.

30. Hansen S, Anderson M, Cornett C, Gradinaru R, Grunnet N: **A role for taurine in mitochondrial function**. *Journal of Biomedical Science* 2010, **17**(S23):1-8.

31. Zulli A: **Taurine in cardiovascular disease**. *Current Opinion in Clinical Nutrition & Metabolic Care* 2011, **14**(1):57-60.

32. Chen G, Nan C, Tian J, Jean-Charles P, Li Y, Weissbach H, Huang XP: **Protective effects of taurine against oxidative stress in the heart of MsrA knockout mice**. *Journal of Cellular Biochemistry* 2012, **113**(11):3559-3566.

33. Olson JE, Martinho EJ: **Taurine transporter regulation in hippocampal neurons**. *Advances in Experimental Medicine and Biology* 2006, **583**:307-314.

34. Hernández-Benítez R, Pasantes-Morales H, Saldaña IT, Ramos-Mandujano G: **Taurine stimulates proliferation of mice embryonic cultured neural progenitor cells**. *Journal of Neuroscience Research* 2010, **88**(8):1673-1681.

35. Fordahl SC, Anderson JG, Cooney PT, Weaver TL, Colyer CL, Erikson KM: **Manganese exposure inhibits the clearance of extracellular GABA and influences taurine homeostasis in the striatum of developing rats**. *Neurotoxicology* 2010, **31**(6):639-646.

36. Cunningham RA, Miller RF: **Electrophysiological analysis of taurine and glycine action on neurons of the mudpuppy retina. II. ERG, PNR and Müller cell recordings**. *Brain Research* 1980, **197**(1):139-151.

37. Hernández-Benítez R, Ramos-Mandujano G, Pasantes-Morales H: **Taurine stimulates proliferation and promotes neurogenesis of mouse adult cultured neural stem/progenitor cells**. *Stem Cell Research* 2012, **9**(1):24-34.

38. Young TL, Matsuda T, Cepko CL: **The noncoding RNA taurine upregulated gene1 is required for differentiation of the murine retina**. *Current Biology* 2005, **15**(6):501-512.

39. Miller S, Steinberg RH: **Transport of taurine, L-methionine and 3-o-methyl-D-glucose across frog retinal pigment epithelium**. *Experimental Eye Research* 1976, **23**(2):177-189.

40. Hillenkamp J, Hussain AA, Jackson TL, Constable PA, Cunningham JR, Marshall J: **Compartmental analysis of taurine transport to the outer retina in the bovine eye**. *Invest Ophthalmol Vis Sci* 2004, **Nov 45**(11):4099-4105.

41. Sirdah MM: **Protective and therapeutic effectiveness of taurine in diabetes mellitus: A rationale for antioxidant supplementation**. *Diebetes & Metabolic Syndrome: Clinical Research & Reviews* 2015, **9**:55-64.

42. Nandhini AA, Thirunavukkarasu V, Anuradha CV: **Potential role of kinins in the effects of taurine in high-fructose-fed rats**. *Canadian Journal of Physiology and Pharmacology* 2004, **82**(1):1-8.

43. Nandhini AA, Anuradha CV: **Taurine modulates kallikrein activity and glucose metabolism in insulin resistant rats**. *Amino Acids* 2002, **22**(1):27-38.

44. Nandhini AA, Thirunavukkarasu V, Anuradha CV: **Taurine modifies insulin signaling enzymes in the fructose-fed insulin resistant rats**. *Diabetes & Metabolism,* 2005, **31**(4):337-344.

45. Aruoma OI, Halliwell B, Hoey BM, Butler J: **The antioxidant action of taurine, hypotaurine and their metabolic precursors**. *Biochemical Journal* 1988, **256**(1):251-255.

46. Schaffer SW, Azuma J, Mozaffari M: **Role of antioxidant activity of taurine in diabetes**. *Canadian Journal of Physiology and Pharmacology* 2009, **87**(2):91-99.

47. Kontny E, Szczepańska K, Kowalczewski J, Kurowska M, Janicka I, Marcinkiewicz J, Maśliński W: **The mechanism of taurine chloramine inhibition of cytokine (interleukin-6, interleukin-8) production by rheumatoid arthritis fibroblast-like synoviocytes**. *Arthritis & Rheumatology* 2000, **43**(10):2169-2177.

48. Franconi F, Di Leo MA, Bennardini F, Ghirlanda G: **Is taurine beneficial in reducing risk factors for diabetes mellitus?** . *Neurochemical Research* 2004, **29**(1):143-150.

49. Marcinkiewicz J, Kontny E: **Taurine and inflammatory diseases**. *Amino Acids* 2014, **46**:7-20.

50. Jong CJ, Azuma J, Schaffer S: **Mechanism underlying the antioxidant activity of taurine: prevention of mitochondrial oxidant production**. *Amino Acids* 2012, **42**(6):2223-2232.

51. Hayes KC, Carey RE, Schmidt SY: **Retinal degeneration associated with taurine efficiency in the cat**. *Science* 1975, **188**(4191):949-951.

52. Schuller-Levis G, Mehta P, Rudelli R, Sturman J: **Immunological consequences of taurine deficiency in cats**. *Journal of Leukocyte Biology* 1990, **47**:321-331.

53. Holmes RP, Goodman HO, Shihabi ZK, Jarow JP: **The Taurine and Hypotaurine Content of Human Semen**. *Journal of Andrology* 1992, **11**:289-292.

54. Cavallini D, Scandurra R, Dupre S, Santoro L, Barra D: **A new pathway of taurine biosynthesis**. *Physiological Chemistry and Physics* 1976, **8**(2):157.

55. Sumizu K: **Oxidation of hypotaurine in rat liver**. *Biochimica et Biophysica Acta* 1962, **63**:210-212.

56. Fiori A, Costa M: **Oxidation of hypotaurine by peroxide**. *Acta Vitamin (Milano)* 1969, **23**:204-207.

57. Oja SS, Karvonen ML, Lähdesmäki P: **Biosynthesis of taurine and enhancement of decarboxylation of cysteine sulphinate and glutamate by the electrical stimulation of rat brain slices**. *Brain Research* 1973, **55**:173-178.

58. Di Giorgio RM, Macaione S, De Luca G: **Subcellular distribution of hypotaurine oxidase activity in ox retina**. *Life Sciences* 1977, **20**(10):1657-1662.

59. Oja SS, Kontro P: **Oxidation of hypotaurine in vitro by mouse liver and brain tissues**. *Biochimica et Biophysica Acta (BBA)-General Subjects* 1981, **677**(3-4):350-357.

60. Mulligan MK, Mozhui K, Prins P, Williams RW: **GeneNetwork: A toolbox for systems genetics**. *Systems Genetics: Methods and Protocols* 2017:75-120.

61. Okamura Y, Aoki Y, Obayashi T, Tadaka S, Ito S, Narise T, Kinoshita K: **COXPRESdb in 2015: coexpression database for animal species by DNA-microarray and RNAseq-based expression data with multiple quality assessment systems**. *Nucleic Acids Research* 2014, **43**(D1):D82-D86.

62. Krueger SK, Williams DE: **Mammalian flavin-containing monooxygenases: structure/function, genetic polymorphisms and role in drug metabolism**. *Pharmacology & Therapeutics* 2005, **106**(3):357-387.

63. Green TR, Fellman JH, Eicher AL, Pratt KL: **Antioxidant role and subcellular location of hypotaurine and taurine in human neutrophils**. *Biochimica et Biophysica Acta (BBA) - General Subjects* 1991, **1073**:91-97.

64. Winterbourn C, Brennan S: **Characterization of the oxidation products of the reaction between reduced glutathione and hypochlorous acid**. *Biochem J,* 1997, **326**:87-92.

65. Sakakibara S, Yamaguchi K, Hosokawa Y, Kohashi N, Ueda I: **Purification and some properties of rat liver cysteine oxidase (cysteine dioxygenase)**. *Biochimica et Biophysica Acta* 1976, **422**:273-279.

66. Sorbo B, Heyman T: **On the purification of cysteinesulfinic acid decarboxylase and its substrate specificity**. *Biochimica et Biophysica Acta* 1957, **23**:624-627.

67. Liu P, Ge X, Ding H, Jiang H, Christensen BM, Li J: **Role of Glutamate Decarboxylase-like Protein 1 (GADL1) in Taurine Biosynthesis**. *Journal of Biological Chemistry,* 2012, **287**:40898-40906.

68. Cavallini D, De Marco C, Scandurra R, Dupré S, Graziani MT: **The Enzymatic Oxidation of Cysteamine to Hypotaurine**. *Journal of Biological Chemistry* 1966, **241**:3189-3196.

69. Vitvitsky V, Garg SK, Banerjee R: **Taurine Biosynthesis by Neurons and Astrocytes**. *Journal of Biological Chemistry* 2011, **286**:32002-32010.

70. Zinellu A, Sotgia S, Loriga G, Deiana L, Ercole Satta A, Carru C: **Oxidative stress improvement is associated with increased levels of taurine in CKD patients undergoing lipid-lowering therapy**. *Amino Acids* 2012, **43**:1499-1507.

71. Ortega JA, Ortega JM, Julian D: **Hypotaurine and sulfhydryl-containing antioxidants reduce H2S toxicity in erythrocytes from a marine invertebrate**. *Journal of Experimental Biology* 2008, **211**:3816-3825.

72. Fontana M, Giovannitti F, Pecci L: **The protective effect of hypotaurine and cysteine sulphinic acid on peroxynitrite-mediated oxidative reactions**. *Free Radical Research* 2008, **42**:320-330.

73. Lin-Vien D, Colthup NB, Fateley WG, Grasselli JG: *The Handbook of Infrared and Raman Characteristic Frequencies of Organic Molecules* 1991, **Academic Press, Boston**.

74. Schmidt MW, Baldridge KK, Boatz JA, Elbert ST, Gordon MS, Jensen JH, Koseki S, Matsunaga N, Nguyen KA, Su S *et al*: **General Atomic and Molecular Electronic Structure System**. *J Comput Chem* 1993, **14**:1347-1363.

75. Gordon MS, Schmidt MW: **In Dykstra, C.E., Frenking, G., Kim, K.S., andScuseria, G.E. (eds.)**. *Theory and Applications of Computational Chemistry: the first forty years* 2005, **Elsevier, Amsterdam**:1167-1189.

76. Halliwell B, Gutteridge JMC: *Free Radicals in Biology and Medicine, 3rd ed* 2005, **Oxford University Press, London**.

77. Sato S, Higuichi S, Tanaka S: **Identification and Determination of Oxygen-Containing Inorganosulfur Compounds by Laser Raman Spectroscopy**. *Applied Spectroscopy* 1985, **39**:822-827.

78. Halliwell B: **Free Radicals and Antioxidants: A Personal View**. *Nutrition Reviews* 1994, **52**:253-265.

79. Tadolini B, Pintus G, Pinna GG, Bennardini F, Franconi F: **Effects of Taurine and Hypotaurine on Lipid Peroxidation**. *Biochemical and Biophysical Research Communications* 1995, **213**:820-826.

80. Ting-Beall HP, Needham D, Hochmuth RM: **Volume and Osmotic Properties of Human Neutrophils.** . *Blood Journal* 1993, **81**:2774-2780.

81. Vitvitsky V, Martinov M, Ataullakhanov F, Miller RA, Banerjee R: **Sulfur-based redox alterations in long-lived Snell dwarf mice.** . *Mechanisms of Ageing and Development* 2013, **134**:321-330.

82. Baseggio Conrado A, Pecci L, Capuozzo E, Fontana M: **In Marcinkiewicz, J. and Schaffer, W. S. (eds.)**. *Taurine 9 Springer International Publishing, Cham* 2015:41-51.

83. Stipanuk MH, Jurkowska H, Roman HB, Niewiadomski J, Hirschberger LL: **In Marcinkiewicz, J. and Schaffer, W. S. (eds.),** . *Taurine 9 Springer International Publishing, Cham*, 2015:29-39.

84. Pecci L, Costa M, Montefoschi G, Antonucci A, Cavallini D: **Oxidation of hypotaurine to taurine with photochemically generated singlet oxygen: the effect of azide**. *Biochemical and Biophysical Research Communications* 1999, **254**(3):661-665.

85. Grove RQ, Karpowicz SJ: **Reaction of hypotaurine or taurine with superoxide produces the organic peroxysulfonic acid peroxytaurine**. *Free Radical Biology and Medicine* 2017, **108**:575-584.

86. Simon HU, Haj-Yehia A, Levi-Schaffer F: **Role of reactive oxygen species (ROS) in apoptosis induction**. *Apoptosis* 2000, **5**(5):415-418.

87. Hibbard JU, Pridjian G, Whittington PF, Moawad AH: **Taurine transport in the vitro perfused human placenta**. *Pediatr Res* 1990, **27**:80-84.

88. Derosa MC, Crutchley RJ: **Photosensitized singlet oxygen and its applications**. *Coordination Chemistry Reviews* 2002, **233-243, 351-371**.

89. Brame J, Long M, Li Q, Alvarez P: **Trading oxidation power for efficiency: Differential inhibition of photo-generated hydroxyl radicals versus singlet oxygen**. *Water Research* 2014, **60**:259-266.

90. Kolthoff IM, Medalia AI: **The reaction between ferrous iron and peroxides. I. Reaction with hydrogen peroxide in the absence of oxygen**. *Journal of the American Chemical Society* 1949, **71**(11):3777-3783.

91. Craig DP, Short LN: **Absorption spectra of acridines. Part I. Some aminoacridines**. *Journal of the Chemical Society (Resumed)* 1945, **0**:419-422.

92. Ryzhakov AV, Nizhnik YP, Andreev VP: **Molecular complexes of acridine N-oxide**. *Russian Journal of Electrochemistry* 2000, **36**(6):884-886.

93. Acheson RM, Adcock B: **The Peroxyacid oxidation of acridine**. *Journal of the Chemical Society C: Organic* 1968:1045-1047.

94. Loures CC, Alcântara MA, Izário Filho HJ, Teixeira ACSC, Silva FT, Paiva TC, Samanamud GR: **Advanced oxidative degradation processes: fundamentals and applications**. *International Review of Chemical Engineering* 2013, **5**(2):102-120.

95. Kataoka H, Ohnishi N, Makita M: **Electron-capture gas chromatography of taurine as its N-pentafluorobenzoyl di-n-butylamide derivative**. *Journal Chromatography B: Biomedical Sciences and Applications* 1985, **339**:370-374.